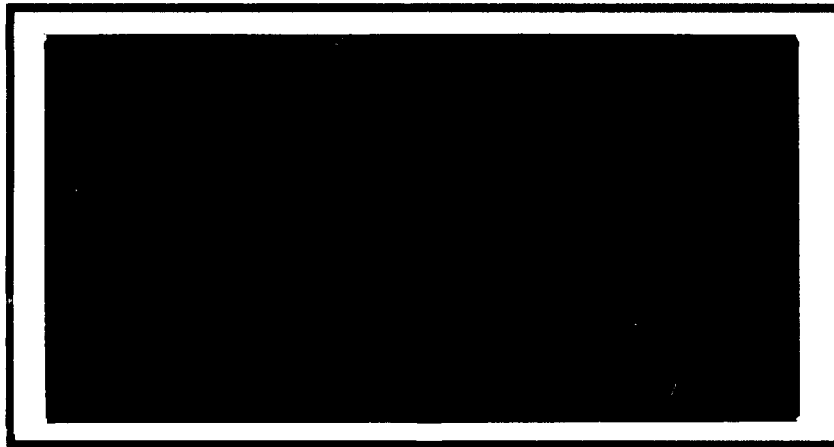


AD-A230 665



DEPARTMENT OF THE AIR FORCE
AIR UNIVERSITY

AIR FORCE INSTITUTE OF TECHNOLOGY

DTIC
ELECTE
JAN 08 1991
S E D

Wright-Patterson Air Force Base, Ohio

DISTRIBUTION STATEMENT A
Approved for public release;
Distribution Unlimited



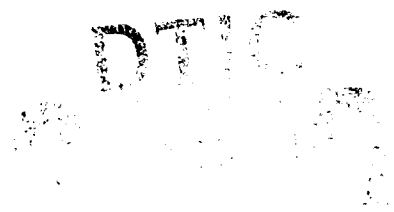
AFIT/GAE/ENY/90D-5

DAMPING OF LAYERED
BEAMS WITH MIXED
BOUNDARY CONDITIONS

THESIS

Eugene T. Cottle
Captain, USAF

AFIT/GAE/ENY/90D-5



Approved for public release; distribution unlimited

DAMPING OF LAYERED BEAMS WITH MIXED BOUNDARY CONDITIONS

THESIS

Presented to the Faculty of the School of Engineering
of the Air Force Institute of Technology
Air University
In Partial Fulfillment of the
Requirements for the Degree of
Master of Science in Aerospace Engineering

Eugene T. Cottle, B.S.

Captain, USAF

Dec, 1990

Accession For	
NTIS GRA&I	<input checked="" type="checkbox"/>
DTIC TAB	<input type="checkbox"/>
Unannounced	<input type="checkbox"/>
Justification	
By _____	
Distribution/	
Availability Codes	
Dist	Avail and/or Special
A-1	

Approved for public release; distribution unlimited



Preface

For the reader who is unfamiliar with viscoelasticity, Chapter III presents a general overview of some basic concepts. It also introduces some of the notation used in the rest of the document. Most of Chapter IV could also be considered introductory, since the presentation doesn't depart from well-established theory until about the end of the chapter.

The symbol list was cumbersome enough that I included it as Appendix A, rather than in the prefatory pages. The notation there appears roughly in the same order in which it is introduced in the text. Most symbols are also defined where they are first introduced in the text.

This thesis would not have been possible if I had not received plenty of help and encouragement. My faculty advisor, Dr. Torvik, showed exceptional patience and tolerance. I also received some timely advice from Dr. Jones in the Materials Laboratory, which profoundly affected the final content of the thesis. Of course, my wife and family deserve credit for enduring the long hours, and for shoring up my confidence. My wife has always had more faith in me than I have in myself.

All students in the GAE90D graduating class are sobered by the memory of a classmate who died last year in an automobile accident. Such a tragedy broadens our perspective on school, and on life. May we all keep a keen eye on our priorities.

In memory of Wayne P. Wilsdon.

Eugene T. Cottle

Table of Contents

	Page
Preface	ii
Table of Contents	iii
List of Figures	v
List of Tables	vii
Abstract	viii
I. Introduction	1
II. Historical Perspective	4
III. Preliminary Concepts	6
IV. Derivation of Equations of Motion	13
V. General Solution of the Equations of Motion	19
VI. Boundary Condition Matrices	24
Both Base and Constraining Layers Fixed at $x = 0$, Free at $x = L$	24
Base Layer Fixed at $x = 0$ and Free at $x = L$; Constraining Layer Free at $x = 0$ and at $x = L$	26
Base Layer Pinned at $x = 0$ and at $x = L$; Constraining Layer Free at $x = 0$ and Free at $x = L$	29
Base Layer Pinned at $x = 0$ and at $x = L$; Constraining Layer Rotates with Base Layer at $x = 0$ and Free at $x = L$	30

	Page
VII. Numerical Results	33
Computer Programming Approach	33
Test Cases for Validating Software	36
Case 1 - Bare Beam	36
Case 2 - Rigid Spacer	38
Case 3 - Simply Supported	39
Test Cases Illustrating the Effect of Considering Mixed Boundary Conditions .	46
Comparison of Complex Frequencies for Cantilever Boundary Conditions	46
Comparison of Complex Frequencies for Simply Supported Boundary Conditions	48
Effect of Permitting Mixed Boundary Conditions on Optimum Design .	51
VIII. Recommendations for Further Research	61
IX. Conclusion	62
Appendix A. Notation	63
Appendix B. Description of User Input for BEAM	67
Appendix C. Programming Notes for Program BEAM	73
Bibliography	74
Vita	75

List of Figures

Figure	Page
1. Constrained Layer Damping Treatment	2
2. Normalized Lateral Displacement - Base Layer Pinned-Pinned, Constraining Layer Free-Free	45
3. Normalized Longitudinal Displacement of Base Layer - Base Layer Pinned-Pinned, Constraining Layer Free-Free	46
4. Normalized Longitudinal Displacement of Constraining Layer - Base Layer Pinned-Pinned, Constraining Layer Free-Free	47
5. Complex Frequencies for Cantilever Boundary Conditions	49
6. Normalized Lateral Displacement, All Layers Fixed-Free	49
7. Normalized Longitudinal Displacement of Base Layer, All Layers Fixed-Free	50
8. Normalized Longitudinal Displacement of Constraining Layer, All Layers Fixed-Free	50
9. Normalized Lateral Displacement, Base Layer Fixed Free, Constraining Layer Free Free	51
10. Normalized Longitudinal Displacement of Base Layer, Base Layer Fixed Free, Constraining Layer Free Free	52
11. Normalized Longitudinal Displacement of Constraining Layer, Base Layer Fixed Free, Constraining Layer Free Free	53
12. Complex Frequencies for Simply Supported Boundary Conditions	53
13. Normalized Lateral Displacement, Base Layer Simply Supported, Constraining Layer Rigid-Free	54
14. Normalized Longitudinal Displacement of Base Layer, Base Layer Simply Supported, Constraining Layer Rigid-Free	55
15. Normalized Longitudinal Displacement of Constraining Layer, Base Layer Simply Supported, Constraining Layer Rigid-Free	56
16. Beam Loss Factor vs. Thickness as Predicted by PREDY - All Layers Fixed-Free	56
17. Beam Loss Factor vs. Thickness as Predicted by BEAM - All Layers Fixed-Free	57
18. Beam Loss Factor vs. Thickness as Predicted by BEAM - Base Layer Fixed-Free, Constraining Layer Free-Free	57

Figure	Page
19. Beam Loss Factor vs. Thickness as Predicted by BEAM - Base Layer Simply Supported, Constraining Layer Free-Free	58
20. Beam Loss Factor vs. Thickness as Predicted by BEAM - Base Layer Simply Supported, Constraining Layer Rigid-Free	59
21. Beam Loss Factor vs. Thickness as Predicted by BEAM - Comparison of Cantilever Boundary Conditions, Mode 4	60

List of Tables

Table	Page
1. Summary of Boundary Conditions Considered	24
2. Basic Data Used as Starting Point for All Test Cases	34
3. Data Used to Calculate Theoretical Frequencies for Cases 1 and 2	37
4. Input Data for Program BEAM for Cases 1 and 2	38
5. Case 1 - Comparison of Bare Beam Theoretical Frequencies with Values Predicted by BEAM	38
6. Case 2 - Comparison of Rigid Spacer Theoretical Frequencies with Values Predicted by BEAM	39
7. BEAM Output, Test Case 3, Mode 1	42
8. Conditions on Constants A and γ - Case 3 Mode 1	43
9. BEAM Output, Test Case 3, Mode 2	44
10. Conditions on Constants A and γ - Case 3 Mode 2	44
11. Values of Complex Frequency Predicted by BEAM and PREDY for Cantilever Bound- ary Conditions	48
12. Complex Frequencies Predicted by BEAM for Simply Supported Boundary Conditions	48
13. Approximate Adhesive Layer Thicknesses for Optimum Damping - Cantilever Bound- ary Conditions (meters)	55
14. Approximate Adhesive Layer Thicknesses for Optimum Damping - Simply Supported Boundary Conditions (meters)	55

Abstract

For many years, viscoelastic materials have been used in damping treatments to control vibration. In order to optimize a damping treatment for maximum damping, a design engineer must be able to predict frequencies of vibration of damped normal modes and loss factors as a function of the design parameters. Theoretical models of layered beams have been developed, but to date, exact solutions have assumed boundary conditions to be the same for all layers.

In this thesis, equations of motion for a damped, layered beam are solved for the longitudinal displacement of both elastic layers, as well as the lateral displacement of the composite beam. Test cases were run on a computer to verify the validity of the equations, and to compare results with previously published approximate methods. Results show that the software compares well with theory for cases in which simple theoretical solutions are available.

JS

To determine the effect of mixed boundary conditions on design optimization, the system damping factor was calculated as a function of adhesive layer thickness using both the previously published approximate methods and the new formulation. Permitting mixed boundary conditions was shown to significantly effect design optimization.

DAMPING OF LAYERED BEAMS WITH MIXED BOUNDARY CONDITIONS

I. Introduction

Engineers frequently face the problem of excessive vibration in structures, especially in the aerospace industry. One approach to eliminating or reducing excessive vibration is to use materials which tend to dampen vibration. Materials can be designed into the structure, or they can be added to an existing structure. The latter approach is more common, since vibration problems usually only show up after the structure is put into service. Damping materials are commonly added to a structure in the form of a damping tape. Damping tape is a viscoelastic adhesive on a foil substrate.

A design engineer is interested in maximizing system damping for a structure. In order to maximize damping, it is necessary to calculate the damping as a function of the design parameters. The system damping is a function of the frequency of vibration of steady state harmonic motion. To calculate system damping, then, it is necessary to solve the equations of motion of the structure of interest for the damped normal modes and resonant frequencies. Theoretical models of damped structures have been developed (18), and the literature suggests that optimum configurations exist (13).

One of the structures which has been investigated extensively is a layered beam. A schematic of a layered beam is shown in Figure 1. It consists a base layer, generally the structure of interest, covered by a viscoelastic layer and an elastic constraining layer. The constraining layer induces high shear strains in the adhesive layer. The shear strain in the viscoelastic layer is the primary damping mechanism (7).

Solutions to the equations of motion of the layered beam have considered boundary conditions only on the composite beam (13). In other words, the boundary conditions for all layers are the

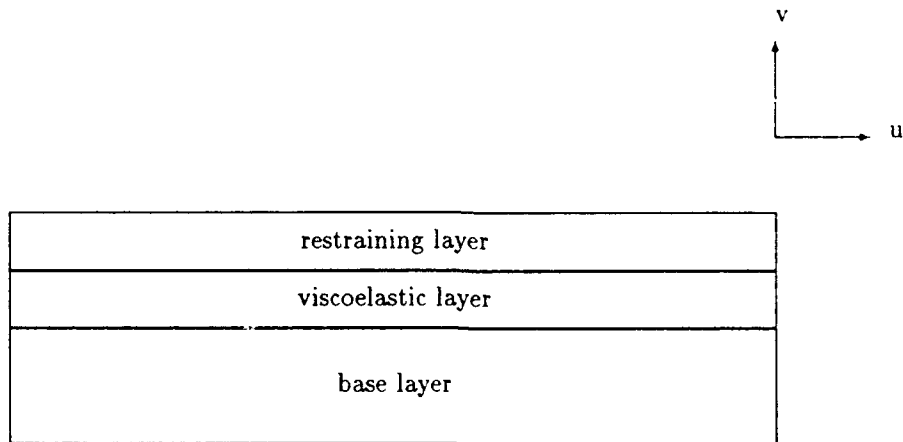


Figure 1. Constrained Layer Damping Treatment

same. However, in practice, it is likely that the layers of the damped structure will not have the same boundary conditions. The question which needs to be answered, then, is how would the calculation of an optimum system design be affected by permitting the boundary conditions of a layered beam to be different for the individual layers.

In this thesis, the equations of motion are solved and system damping are calculated for a layered beam in which the elastic layers are permitted to have different boundary conditions. The effect of permitting mixed boundary conditions on the optimum system design is investigated.

A brief historical overview is first presented to show how the present work relates to previously published theoretical work. Following the historical overview, the reader is introduced to some of the basic concepts of viscoelastic damping. The equations of motion are then derived using Hamilton's principle (9:44). The boundary conditions are shown, and boundary condition matrices are shown for several important cases.

Numerical results are presented which demonstrate the validity of the equations and software, and which illustrate the effect of considering mixed boundary conditions on the optimum design.

Some of the factors which were considered in programming the equations are discussed briefly. Test cases are considered for which simple solutions existed. It is shown that the complex frequencies predicted by the software compare well with the results predicted by the simple theory. Complex frequencies and mode shapes are shown which illustrate the effect of considering mixed boundary conditions. In addition to mode shapes of lateral vibration of the composite beam, mode shapes of longitudinal vibration of the elastic layers are also shown. Finally, sample optimization curves are shown. Damping is calculated as a function of adhesive layer thickness for several cases. It is shown that the formulation presented here predicts an order of magnitude different optimum thickness than do previously published approximate methods. It is also shown that considering mixed boundary conditions significantly affects the optimum design.

II. Historical Perspective

There have been literally hundreds of theoretical treatments of viscoelastic damping mechanisms over the past four decades. There have also been comprehensive literature reviews by recognized experts in the field (18). This perspective will review only what might be considered milestones in the theoretical development, and consider the general trends in the research, particularly as it concerns the subject of this thesis.

For a number of years before a theoretical treatment was available, viscoelastic material had been used as a damping treatment in the form of damping tape (7). The damping tape consisted of viscoelastic material on a foil substrate.

Governing equations for structures with a constrained viscoelastic layer were presented by Kerwin in 1958, who cited earlier theoretical work by Oberst and Licnard (7). The viscoelastic characteristics of a material were modelled by permitting the shear modulus to take on complex values. Kerwin identified shear strain as the primary damping mechanism in a layered beam. DiTaranto (5) solved the sixth order auxiliary equation for longitudinal displacement of the beam. Mead and Markus (8) reformulated the equations in terms of the lateral displacement of the beam, listed possible boundary conditions, and demonstrated orthogonality of damped normal modes. In this early research, while a broad category of boundary conditions were acknowledged, solutions were restricted to the simply supported case. More complicated boundary conditions presented numerical difficulties (13). It is also important to note that boundary conditions were considered on the composite beam, but not on individual elastic layers.

In 1978, Trompette et al (20) presented a finite element solution for the problem of mixed boundary conditions. At about the same time, Rao (13) presented theoretical solutions and exact frequencies and loss factors for all possible boundary conditions on the composite beam. Rao also presented approximate formulae which satisfactorily approximated the exact solutions for material loss factor ≤ 0.3 .

During the past decade, several important theoretical advances were made. Bagley and Torvik (2) introduced fractional calculus models for transient analysis of viscoelastically damped structures. Simply stated, fractional calculus permits differentiation and integration of arbitrary order rather than just of integer order. In other words, a derivative may be represented by $d^\lambda f/dx^\lambda$, where λ is not restricted to integer values. Miles and Reinhall (11) included effects of thickness deformation of the adhesive layer. Finally, Torvik (19) derived the equations of motion and boundary conditions for a multiple layered configuration in which the longitudinal displacements of the elastic layers are considered separately. That treatment laid the groundwork for an exact solution in which mixed boundary conditions are permitted.

This thesis uses an approach similar to Rao (13) to solve the equations of motion presented by Torvik (19) for lateral displacement of the composite beam, as well as for longitudinal displacements of the separate elastic layers. The approach can be generalized to multiple layers as was suggested by Torvik (19).

III. Preliminary Concepts

A brief explanation of viscoelasticity will be presented, to familiarize the reader with basic concepts and notation used in the rest of the document. The loss factor is defined, and a distinction is made between the material loss factor and the beam equivalent loss factor.

The stress-strain relation for a one dimensional, linear, elastic material is generally represented by (6:89)

$$\sigma = E\epsilon \quad (1)$$

where

σ = stress

ϵ = strain

E = Young's modulus, an experimentally determined proportionality constant

Material *viscoelasticity*, in contrast to *elasticity*, permits the relationship to include dependence not only on stress and strain, but on stress rates and strain rates (3:14-25). For example, one simple model of viscoelasticity, called the Kelvin or Voigt model, for an isotropic material, could be written

$$\sigma = E_1\epsilon + E_2\frac{d\epsilon}{dt} \quad (2)$$

where

E_1 and E_2 = experimentally determined proportionality constants

t = time

The dependence of stress on the strain rate is called 'creep', because, for a constant stress, the strain continues to change with time. This can be seen by solving Eqn 2 for ϵ as a function of σ and t . In a similar way, strain can be related to stress rate. Stress rate dependence is called 'relaxation', because it permits stress to change with time while strain is held constant.

A more general model could be expected to include not only a dependence on the first derivatives of stress or strain with respect to time, but on higher order derivatives as well. The stress-strain relationship for a general, one dimensional, linear viscoelastic material could be written (3:14)

$$\sum_{m=0}^M a_m \frac{d^m \sigma}{dt^m} = \sum_{n=0}^N b_n \frac{d^n \epsilon}{dt^n} \quad (3)$$

where

a_m and b_n = empirical proportionality constants

M and N = the number of derivatives and proportionality constants considered

For a simple elastic material, $M = N = 0$. In the Kelvin model, $M = 0$ and $N = 1$. While Eqn 3 shows dependence on integer derivatives, it is also possible to consider a dependence involving fractional derivatives (2). In other words, m and n need not be integers.

For steady state oscillatory motion, the stress and strain can be represented by periodic functions of time (3:21):

$$\sigma = \sigma_0 e^{i\omega t} \quad \text{and} \quad \epsilon = \epsilon_0 e^{i\omega t} \quad (4)$$

where

σ_0 = average stress

ϵ_0 = average strain

ω = complex frequency

Substituting equations 4 into Eqns 3 results in two complex polynomials in frequency. Factoring σ_0 and ϵ_0 from the polynomials, and dividing through by the polynomial on the left side of the equation, yields

$$\sigma_0 = \frac{\sum_{n=0}^N b_n (i\omega)^n}{\sum_{m=0}^M a_m (i\omega)^m} \epsilon_0 \quad (5)$$

which is of the form

$$\text{complex stress} = \text{complex modulus} \times \text{complex strain}$$

According to this argument, it is possible to represent the stress-strain relationship of a general, one dimensional, linear viscoelastic material with a single complex modulus, which can be experimentally determined. The modulus will be a function of frequency.

Although Eqn 3 leads to an intuitive feel for meaning of a complex modulus, it will be shown that most materials cannot be represented by a linear model with integer derivatives. Fortunately, the concept of a complex modulus is still valid for more complicated constitutive relations. Reference (3) gives a more rigorous treatment.

In analyses of viscoelastic damping treatments, the shear modulus of the adhesive layer is generally taken to be complex (7), of the form $G(1 + i\eta_v)$. The term η_v is called the loss factor of the material. The subscript v will be used to differentiate between the loss factor of the viscoelastic material, and the equivalent loss factor of the composite beam. The beam loss factor will be denoted η_b , and is explained below. Note that η_v is the ratio of the imaginary and real parts of the complex modulus. The real and the imaginary parts of the complex modulus are called the storage and loss moduli, respectively (3:22).

Although typically only the shear modulus of the adhesive layer is considered complex, the elastic modulus may also be complex. This concept may be used to analyze multi-layered beams (19). The treatment in the chapters which follow, and the software developed under this effort, permit a complex elastic modulus.

The loss factors of important damping materials have been experimentally determined and characterized in a damping design guide published in 1985 (17). Data in the design guide is presented in a graphical format called a reduced temperature nomogram (17:1-13,503-511). A designer can either read damping data from the nomogram, or calculate it using an analytical representation. The analytical representation is a curve fit of the experimental data. To use the analytical representation, the designer first calculates a reduced temperature, called α_T , then uses the reduced temperature to calculate the complex frequency, from the following formulae:

$$\log \alpha_T = a \left[\frac{1}{T} - \frac{1}{A(1)} \right] + 2.303 \left(\frac{2a}{A(1)} - b \right) \log \left(\frac{T}{A(1)} \right) + \left[\frac{b}{A(1)} - \frac{a}{A(1)^2} - A(4) \right] (T - A(1)) \quad (6)$$

where

$$T = \text{temperature}$$

$$a = (D_B C_C - C_B D_C) / D_E$$

$$b = (C_A D_C - D_A C_C) / D_E$$

$$C_A = \left[\frac{1}{A(2)} - \frac{1}{A(1)} \right]^2$$

$$C_B = \frac{1}{A(2)} - \frac{1}{A(1)}$$

$$C_C = A(5) - A(4)$$

$$D_A = \left[\frac{1}{A(3)} - \frac{1}{A(1)} \right]^2$$

$$D_B = \frac{1}{A(3)} - \frac{1}{A(1)}$$

$$D_C = A(6) - A(4)$$

$$D_E = D_B C_A - C_B D_A$$

$$A(1) \dots A(6) = \text{curve fit parameters specified for material}$$

and

$$G = B(1) + \frac{B(2)}{1 + B(5) [B(3)/(fi)]^{B(6)} + [B(3)/(fi)]^{B(4)}} \quad (7)$$

where

G = Complex shear modulus

i = $\sqrt{-1}$

f = frequency

$B(1) \dots B(6)$ = curve fit parameters specified for material

The temperature and frequency should be specified in units which are consistent with the parameters $A(1) \dots A(6)$ and $B(1) \dots B(6)$. Note that in Eqn 7 the complex modulus is not a simple ratio of polynomials in frequency, as suggested by Eqn 3. As mentioned earlier, this does not invalidate the concept of a complex modulus. It only suggests that most materials cannot be adequately represented by the linear constitutive relation in integer derivatives. The derivation in the following chapters permits the modulus to be a function of frequency, but does not make any assumptions regarding the functional form of that dependence.

There are a number of ways to quantify the damping of a system. They include the loss factor, percent critical damping, viscous damping factor, log decrement, complex frequency, etc. All these quantities are related (15:2-7). To avoid the inevitable confusion, only two quantities will be used in this thesis. One will be the complex damped natural frequency of vibration:

$$\omega = \omega_R + \omega_I i \quad (8)$$

where

ω = complex frequency of vibration

ω_R = real part of the complex frequency

ω_I = imaginary part of the complex frequency

The other will be the loss factor η . The distinction between the beam loss factor, η_b , and the material loss factor η_v , will be made in a moment.

The relationship between the loss factor and the complex frequency can be seen by solving the equation of motion of a second order system. The equation of motion of free vibration of an undamped harmonic oscillator is (10:19)

$$m\ddot{u} + ku = 0 \quad (9)$$

where

m = mass

u = displacement

k = spring constant or elastic modulus

Damping can be introduced into the equation by letting the spring constant be complex:

$$m\ddot{x} + k(1 + i\eta)x = 0 \quad (10)$$

This is solved in the standard fashion, by assuming $x = e^{i\omega t}$, noting that ω may be complex. After some simple manipulation, it can be shown that

$$(1 + i\eta) = \frac{m}{k} (\omega_R^2 - \omega_I^2 + 2\omega_R\omega_I i) \quad (11)$$

Equating the imaginary parts leads to a relationship between the loss factor and the complex frequency:

$$\eta = \frac{2\omega_R\omega_I}{\omega_R^2 - \omega_I^2} \quad (12)$$

or

$$\eta \approx \frac{2\omega_I}{\omega_R} \quad \text{for} \quad \omega_I \ll \omega_R \quad (13)$$

For a homogeneous beam, the loss factor is simply the loss factor of the material. However, for the layered beam, the loss factor defined by Eqn 12, will, in general, be different than the loss factor of the material in the adhesive layer. For this reason, subscripts will be used to differentiate between the two. The loss factor of the material will be called η_v , and the loss factor of the beam, defined by Eqn 12, will be called η_b .

The preliminary concepts which have been shown here are enough to permit us now to derive the equations of motion of a layered beam.

IV. Derivation of Equations of Motion

The equations of motion will be derived for a three-layer beam using Hamilton's principle (9:44). To apply Hamilton's principle, it is necessary to first find expressions for the kinetic and potential energy. This derivation is similar to work which can be found in the literature (8) (13). It will be shown how the equations of motion differ from previous work.

Since the goal is to calculate 'damped normal modes' (8), the derivation which follows will consider only the homogeneous case, i.e. externally applied loads will not be included in the potential energy terms.

Figure 1 shows the directions of the lateral displacements, v , and the longitudinal displacements, u . Lateral displacements are perpendicular to the axis of the beam, and longitudinal displacements are along the axis of the beam. Only the plane strain case will be considered (14:220). Plane strain implies that displacements 'out of the page' are zero.

The kinetic energy of the beam is

$$T = \int_0^L \left\{ \frac{1}{2} \rho_{e0} b t_{e0} (\dot{v}_{e0}^2 + \dot{u}_{e0}^2) + \frac{1}{2} \rho_{e1} b t_{e1} (\dot{v}_{e1}^2 + \dot{u}_{e1}^2) + \frac{1}{2} \rho_{v1} b t_{v1} \left[\dot{v}_{e0}^2 + \left(\frac{\dot{u}_{e0} + \dot{u}_{e1}}{2} \right)^2 \right] \right\} dx \quad (14)$$

where

- L = length of the beam
- b = width of the beam
- ρ_{e0} = density of base (elastic) layer
- t_{e0} = thickness of the base layer
- v_{e0} = lateral displacement of the base layer
- u_{e0} = longitudinal displacement of the base layer
- ρ_{v1} = density of 1st viscoelastic layer
- t_{v1} = thickness of the 1st viscoelastic layer
- v_{v1} = lateral displacement of the 1st viscoelastic layer
- u_{v1} = longitudinal displacement of the 1st viscoelastic layer
- ρ_{e1} = density of 1st elastic layer
- t_{e1} = thickness of the 1st elastic layer
- v_{e1} = lateral displacement of the 1st elastic layer
- u_{e1} = longitudinal displacement of the 1st elastic layer

Kinetic energy of rotation is assumed to be negligibly small in Eqn 14. This is reasonable when displacements are small compared to the length of the beam. Eqn 14 can be simplified by assuming the and the kinetic energy due to the longitudinal displacements is small compared to that due to lateral displacements. Also assuming $v = v_{e0} = v_{e1}$, and assuming unit width, $b = 1$, reduces the kinetic energy to

$$T = \int_0^L \frac{1}{2} (\rho t)_T \left(\frac{\partial v}{\partial t} \right)^2 dx \quad (15)$$

where

$$(\rho t)_T = \rho_{e0} t_{e0} + \rho_{e1} t_{e1} + \rho_{v1} t_{v1} \quad (16)$$

is the equivalent areal density (mass per unit area) of the beam.

The potential energy is

$$V = \int_0^L \frac{1}{2} \left[D_T \left(\frac{\partial^2 v}{\partial^2 x} \right)^2 + E_{e0} t_{e0} \left(\frac{\partial u_{e0}}{\partial x} \right)^2 + E_{e1} t_{e1} \left(\frac{\partial u_{e1}}{\partial x} \right)^2 + G_{v1} t_{v1} \gamma_{v1}^2 \right] dx \quad (17)$$

where

E_{e0} = modulus of elasticity of the base (elastic) layer

G_{v1} = shear modulus of the 1st viscoelastic layer

E_{e1} = modulus of elasticity of the 1st elastic layer

and

$$\gamma_{v1} = \frac{u_{e1} - u_{e0}}{t_{v1}} + d_1 \frac{\partial v}{\partial x} \quad (18)$$

$$d_1 = 1 + \frac{t_{e1} + t_{e0}}{2t_{v1}} \quad (19)$$

$$D_T = \frac{E_{e0} t_{e0}^3}{12(1 - \nu_{e1}^2)} + \frac{E_{e1} t_{e1}^3}{12(1 - \nu_{e1}^2)} \quad (20)$$

It has been assumed (5) (8) that

$$G_{v1} t_{v1} \gamma_{v1}^2 \gg G_{e0} t_{e0} \gamma_{e0}^2 + G_{e1} t_{e1} \gamma_{e1}^2 \quad (21)$$

$$E_{v1} t_{v1} \left[\frac{1}{2} \left(\frac{\partial u_{e1}}{\partial x} + \frac{\partial u_{e0}}{\partial x} \right) \right]^2 \ll E_{e0} t_{e0} \left(\frac{\partial u_{e0}}{\partial x} \right)^2 + E_{e1} t_{e1} \left(\frac{\partial u_{e1}}{\partial x} \right)^2 \quad (22)$$

Eqn 21 states that the shear strain energy in the elastic layers is small compared to the shear strain energy of the adhesive layer. This is reasonable since the damping treatment is inducing large shear strains in the adhesive layer. Eqn 22 states that the strain energy in the adhesive layer due to longitudinal displacement is small compared to the longitudinal strain energies of the elastic layers. This is reasonable since the longitudinal strain of the adhesive layer cannot be greater than the strains in the elastic layers, and the elastic modulus of the adhesive layer will be small compared to the elastic layers.

Hamilton's principle (9:44) requires:

$$\begin{aligned}
& \int_{t_1}^{t_2} (\delta T - \delta V) dt = \\
& \int_{t_1}^{t_2} \int_0^L \left[(\rho t)_T \frac{\partial v}{\partial t} \delta \left(\frac{\partial v}{\partial t} \right) - D_T \frac{\partial^2 v}{\partial x^2} \delta \left(\frac{\partial^2 v}{\partial x^2} \right) - E_{e_0} t_{e_0} \left(\frac{\partial u_{e_0}}{\partial x} \right) \delta \left(\frac{\partial u_{e_0}}{\partial x} \right) - \right. \\
& \left. E_{e_1} t_{e_1} \left(\frac{\partial u_{e_1}}{\partial x} \right) \delta \left(\frac{\partial u_{e_1}}{\partial x} \right) - G_{v_1} t_{v_1} \gamma_{v_1} \delta \gamma_{v_1} \right] dx dt = 0 \tag{23}
\end{aligned}$$

where δ is the variational operator (14:442-443).

The equations of motion and boundary conditions are obtained by integrating Eqn 23 by parts. The integration by parts is carried out in such a way that terms involving derivatives of δv , δu_{e_0} and δu_{e_1} are eliminated from the integral, and only terms involving δv , δu_{e_0} and δu_{e_1} themselves remain under the integral. In doing so, terms are extracted from the integral which contain conditions which must be satisfied at t_1 and t_2 , and at $x = 0$ and L . The variations are $= 0$ at t_1 and t_2 . This is equivalent to saying that initial conditions will be specified. The conditions which must be satisfied at $x = 0$ and L are the boundary conditions. They will be listed later. What results from the application of Hamilton's principle and the integration by parts, then, is an integral expression which must be satisfied, and a set of boundary conditions. The integral expression which must be satisfied is

$$\begin{aligned}
& \int_0^L \left\{ (-\rho t)_T \frac{\partial^2 v}{\partial t^2} \delta v - D_T \frac{\partial^4 v}{\partial x^4} \delta v \right. \\
& + E_{e_0} t_{e_0} \frac{\partial^2 u_{e_0}}{\partial x^2} \delta u_{e_0} + E_{e_1} t_{e_1} \frac{\partial^2 u_{e_1}}{\partial x^2} \delta u_{e_1} \\
& - G_{v_1} t_{v_1} \left[\left(\frac{u_{e_1} - u_{e_0}}{t_{v_1}} \right) \left(\frac{\delta u_{e_1} - \delta u_{e_0}}{t_{v_1}} \right) + d_1 \frac{\partial v}{\partial x} \left(\frac{\delta u_{e_1} - \delta u_{e_0}}{t_{v_1}} \right) \right. \\
& \left. - d_1 \frac{\partial}{\partial x} \left(\frac{u_{e_1} - u_{e_0}}{t_{v_1}} \right) \delta v - d_1^2 \frac{\partial^2 v}{\partial x^2} \delta v \right] \left. \right\} dx = 0 \tag{24}
\end{aligned}$$

The integral must be identically 0 for all x . The variations δv , δu_{e0} and δu_{e1} are permitted to vary arbitrarily and independently over the domain (14:445) from $x = 0$ to $x = L$, so the coefficients of the variations inside the integral must all vanish. This leads to the equations of motion:

$$\begin{aligned}
 D_T \frac{\partial^4 v}{\partial v^4} + (\rho t)_T \frac{\partial^2 v}{\partial t^2} - G_{v1} t_{v1} d_1 \left[\frac{1}{t_{v1}} \left(\frac{\partial u_{e1}}{\partial x} - \frac{\partial u_{e0}}{\partial x} \right) + d_1 \frac{\partial^2 v}{\partial x^2} \right] &= 0 \\
 E_{e0} t_{e0} \frac{\partial^2 u_{e0}}{\partial x^2} + G_{v1} \left(\frac{u_{e1} - u_{e0}}{t_{v1}} + d_1 \frac{\partial v}{\partial x} \right) &= 0 \\
 E_{e1} t_{e1} \frac{\partial^2 u_{e1}}{\partial x^2} - G_{v1} \left(\frac{u_{e1} - u_{e0}}{t_{v1}} + d_1 \frac{\partial v}{\partial x} \right) &= 0
 \end{aligned} \tag{25}$$

The boundary conditions were extracted from Eqn 23 during the integration by parts, as conditions which must be satisfied at $x = 0$ or $x = L$. They are

$$\begin{aligned}
 \partial u_{e0} / \partial x &= 0 & \text{or} & & u_{e0} &= 0 \\
 \partial u_{e1} / \partial x &= 0 & \text{or} & & u_{e1} &= 0 \\
 G_{v1} d_1 t_{v1} \left[\frac{u_{e1} - u_{e0}}{t_{v1}} + d_1 \frac{\partial v}{\partial x} \right] - D_T \frac{\partial^3 v}{\partial x^3} & & & & & \\
 &= 0 & \text{or} & & v &= 0 \\
 \partial^2 v / \partial x^2 &= 0 & \text{or} & & \partial v / \partial x &= 0
 \end{aligned} \tag{26}$$

The first of Eqns 26 states that, for the base layer, either the longitudinal displacement must be zero, or the 'slope' of the longitudinal displacement must be zero. Requiring the slope to be zero is equivalent to requiring the end to be force-free. Longitudinal displacement must be unrestrained. The second equation requires the same to be true for the constraining layer. The third equation requires either the lateral displacement of all layers to be zero or be free of shear. It must be either restrained laterally, or free to displace laterally. Note that the expression for the shear force at the end is somewhat more complicated than comparable expressions for homogeneous beams (9:134). It could be considered an equivalent shear force for the composite beam. The last equation requires

either the slope to be zero or the moment to be zero. It must be either prevented from rotating, or free to rotate. These equations must be satisfied at both ends of the beam, so they actually represent a set of eight boundary conditions.

These equations of motion and boundary conditions compare with published results in the early literature (5) (8) (13), except Eqns 26 consider the longitudinal displacements of the elastic layers separately (19). Note that in Eqns 25, u_{e0} and u_{e1} appear only as a difference. Considering boundary conditions on the composite beam is equivalent to considering boundary conditions on the difference between u_{e0} and u_{e1} . In that case, only six equations result (13).

V. General Solution of the Equations of Motion

In the literature (8) (13) (19), Eqns 25 are usually combined into a single sixth order equation. In order to consider mixed boundary conditions, it will be necessary to obtain expressions explicitly for u_{e0} and u_{e1} . This is more easily done if the three separate equations are solved simultaneously. It is possible to obtain the same results by solving the single sixth order equation for v , and substituting the resulting expression back into Eqns 25 to solve for u_{e0} and u_{e1} , but that procedure is more tedious.

Since the problem of interest is steady state oscillatory motion, displacements will be assumed to be periodic functions of time. It is customary (7) (5) (8) to assume a solution of the form

$$\begin{aligned}v &= e^{i\omega t} A e^{px} \\u_{e0} &= e^{i\omega t} B e^{px} \\u_{e1} &= e^{i\omega t} C e^{px}\end{aligned}\tag{27}$$

Note that this assumes the solution is separable. In other words, it assumes that the displacements can be written as a function of x alone times a function of t alone. Assuming a separable solution implies that mode shapes are expected which are not a function of time, as in the steady state. The orthogonality of the solutions (8) guarantees the uniqueness of the steady state solution, but a transient solution of this form may not be unique.

Substituting Eqns 27 into Eqns 25 and dividing through by $e^{i\omega t}$ and e^{px} results in a set of simultaneous algebraic equations. They can be written in matrix form as follows

$$\begin{bmatrix} [D_T p^4 - (\rho t)_T \omega^2 - G_{v1} t_{v1} d_1^2 p^2] & G_{v1} d_1 p & -G_{v1} d_1 p \\ G_{v1} d_1 p & [E_{e0} t_{e0} p^2 - (G_{v1}/t_{v1})] & G_{v1}/t_{v1} \\ -G_{v1} d_1 p & G_{v1}/t_{v1} & [E_{e1} t_{e1} p^2 - (G_{v1}/t_{v1})] \end{bmatrix} \times \begin{bmatrix} A \\ B \\ C \end{bmatrix} = \begin{bmatrix} 0 \\ 0 \\ 0 \end{bmatrix} \quad (28)$$

Finding the solution to Eqns 28 is an eigenvalue problem, although it is not posed in the same general form as most eigenvalue problems (9:138). Still, it can be solved in the same way. A nontrivial solution requires the determinant of the three by three matrix = 0:

$$0 = p^8 - G_{v1} \left[\frac{t_{v1} d_1^2}{D_T} + \frac{1}{t_{v1}} \left(\frac{1}{E_{e1} t_{e1}} + \frac{1}{E_e t_{e0}} \right) \right] p^6 - \frac{\omega^2 (\rho t)_T}{D_T} p^4 + \frac{(\rho t)_T \omega^2 G_{v1}}{D_T t_{v1}} \left(\frac{1}{E_{e1} t_{e1}} + \frac{1}{E_{e0} t_{e0}} \right) p^2 \quad (29)$$

This is the characteristic equation. It differs from the characteristic equation published in the literature (5) (13) in that it has a double zero root. The double zero root is the result of considering longitudinal displacements of the individual elastic layers separately. Note that only even powers of p appear in the equation. This means that the roots will come in pairs. For $p \neq 0$, the roots are found by first solving for the roots of a cubic equation in p^2 , then taking the positive and negative square root of each. The result will be six complex values in positive and negative pairs.

For each value of p which satisfies Eqn 29, Eqns 28 are linearly dependent. For each $p \neq 0$, the solution is determined to within one arbitrary constant. For $p = 0$, the solution is determined to within two arbitrary constants.

The p_j are eigenvalues of the system. Mead and Markus (8) demonstrated that, for $p_j \neq 0$, the associated eigenfunctions are orthogonal. For $p = 0$, the eigenfunctions can be made orthogonal by choosing proper linear combinations of them (9:142). The expansion theorem then guarantees that any function satisfying the homogeneous boundary conditions can be represented as a linear combination of the eigenfunctions (9:143). This means that, for solutions of the form of Eqns 27, the mode shapes will be uniquely determined by a linear combination of the eigenfunctions.

For $p \neq 0$, the eigenfunctions are determined by solving for B and C in terms of A in Eqns 28. Since the equations are now linearly dependent, any two of the equations may be used. Using the first two of Eqns 28 results in the following relation:

$$B_j = \left[\frac{(\rho t)_T \omega^2 - p_j^4 D_T}{t_{v1} d_1 E_{e0} t_{e0} p_j^3} \right] A_j = \beta_j A_j \quad (30)$$

and

$$C_j = \left[\beta_j + \frac{p_j^4 D_T - p_j^2 G_{v1} t_{v1} d_1^2 - (\rho t)_T \omega^2}{G_{v1} d_1 p_j} \right] A_j = \gamma_j A_j \quad (31)$$

If the second and third of Eqns 28 are used, the relations become

$$B_j = \left[\frac{-E_{e1} t_{e1} G_{v1} t_{v1} d_1 p_j}{E_{e0} t_{e0} E_{e1} t_{e1} t_{v1} p_j^2 - G_{v1} (E_{e0} t_{e0} + E_{e1} t_{e1})} \right] A_j = \beta_j A_j \quad (32)$$

and

$$C_j = \left[\frac{E_{e0} t_{e0} G_{v1} t_{v1} d_1 p_j}{E_{e0} t_{e0} E_{e1} t_{e1} t_{v1} p_j^2 - G_{v1} (E_{e0} t_{e0} + E_{e1} t_{e1})} \right] A_j = \gamma_j A_j \quad (33)$$

Eqns 30 and 31 are equivalent to Eqns 32 and 33 for p_j which satisfy Eqn 29. These expressions relate the lateral displacement of the composite beam to the longitudinal displacements of the individual elastic layers.

For $p \neq 0$, there are now only six unspecified constants, $A_1 \dots A_6$. Since there are eight boundary conditions, two more constants are expected. The two additional constants will result from the double zero root in the characteristic equation.

For $p = 0$, the solution is of the form:

$$\begin{aligned}
 v &= e^{i\omega t} (A_7 + A_8 x) \\
 u_{e0} &= e^{i\omega t} (B_7 + B_8 x) \\
 u_{e1} &= e^{i\omega t} (C_7 + C_8 x)
 \end{aligned} \tag{34}$$

Substituting these into Eqns 28 makes the equations linearly dependent. The two independent equations which remain are

$$\begin{aligned}
 -(\rho_T)\omega^2 (A_7 + A_8 x) - G_{v1}d_1 C_8 + G_{v1}d_1 B_8 &= 0 \\
 \frac{G_{v1}}{t_{v1}} (C_7 + C_8 x - B_7 - B_8 x) + G_{v1}d_1 A_8 &= 0
 \end{aligned} \tag{35}$$

Collecting the coefficients of x^0 and x^1 and setting them = 0 yields

$$\begin{aligned}
 -(\rho_T)\omega^2 A_7 - G_{v1}d_1 C_8 + G_{v1}d_1 B_8 &= 0 \\
 \frac{G_{v1}}{t_{v1}} (C_7 - B_7) + G_{v1}d_1 A_8 &= 0 \\
 -(\rho_T)\omega^2 A_8 &= 0 \\
 \frac{G_{v1}}{t_{v1}} (C_8 - B_8) &= 0
 \end{aligned} \tag{36}$$

For $\omega \neq 0$

$$\begin{aligned}
 A_7 = A_8 &= 0 \\
 B_7 &= C_7
 \end{aligned}$$

$$B_8 = C_8$$

For $\omega = 0$, A_7 and A_8 are unspecified (corresponding to rigid body lateral translation and rotation), and

$$B_8 = C_8$$

$$B_7 - C_7 = d_1 t_{v1} A_8$$

If $\omega = 0$ satisfies the boundary conditions, that case must be considered separately. It will not be treated here.

The general solution to Eqns 25 is then

$$\begin{aligned}
 v &= e^{i\omega t} \left[\sum_{j=1}^6 (A_j e^{p_j x}) \right] \\
 u_{e0} &= e^{i\omega t} \left[\sum_{j=1}^6 (\beta_j A_j e^{p_j x}) + B_7 + B_8 x \right] \\
 u_{e1} &= e^{i\omega t} \left[\sum_{j=1}^6 (\gamma_j A_j e^{p_j x}) + B_7 + B_8 x \right]
 \end{aligned} \tag{37}$$

The solution is now determined to within eight arbitrary constants, $A_1 \dots A_6$, B_7 and B_8 . This was to be expected, since there are eight boundary conditions which need to be satisfied. There is also one unspecified parameter, the complex frequency of vibration, ω . It now remains to find the frequency which satisfies a particular set of boundary conditions. Specific boundary condition matrices are considered next.

VI. Boundary Condition Matrices

Substituting Eqns 37 into an appropriate combination of Eqns 26 results in a set of eight simultaneous equations in the eight constants $A_1 \dots A_6$, B_7 and B_8 , and frequency. In matrix form, it can be represented as

$$[\text{boundary condition matrix}] \times \{\text{column vector of coefficients}\} = \{\text{zero vector}\}$$

Nontrivial solutions will exist only when the determinant of the boundary condition matrix is zero. Solving the equations involves finding the complex frequency which drives the determinant to zero. In contrast to the boundary conditions on the composite beam, where the boundary condition matrix is six by six (13), for mixed boundary conditions, in general the matrix will be eight by eight. However, it will be shown that the matrix reduces to a six by six when, at both ends of the beam, the boundary conditions are the same for each elastic layer. In this chapter, boundary condition matrices are presented for several important cases. Boundary conditions were selected which would be most illustrative of the effects of considering the elastic layers separately. A summary of the boundary conditions considered is shown in Table 1. These boundary conditions are used in the numerical results presented in Chapter VII.

Both Base and Constraining Layers Fixed at $x = 0$, Free at $x = L$

The case where both the base and constraining layers fixed at $x = 0$ and free at $x = L$ is of interest because it duplicates solutions which are available in the literature (16:5-24). It will be

Table 1. Summary of Boundary Conditions Considered

Base Layer		Restraining Layer	
$x = 0$	$x = L$	$x = 0$	$x = L$
fixed	free	fixed	free
fixed	free	free	free
pinned	pinned	free	free
pinned	pinned	rigidly connected	free

used for comparison purposes. The boundary conditions are; at $x = 0$

$$\begin{aligned}
 \partial v / \partial x &= 0 \quad \text{zero slope} \\
 v &= 0 \quad \text{zero lateral displacement} \\
 u_{e0} &= 0 \quad \text{zero longitudinal displacement of base layer} \\
 u_{e1} &= 0 \quad \text{zero longitudinal displacement of constraining layer}
 \end{aligned}
 \tag{38}$$

and, at $x = L$

$$\begin{aligned}
 \partial u_{e0} / \partial x &= 0 \quad \text{zero longitudinal force on base layer} \\
 \partial u_{e1} / \partial x &= 0 \quad \text{zero longitudinal force on constraining layer} \\
 \partial^2 v / \partial x^2 &= 0 \quad \text{zero moment on composite beam} \\
 G_{t1} d_1 t_{v1} \left[\frac{u_{e1} - u_{e0}}{t_{v1}} + d_1 \frac{\partial v}{\partial x} \right] - D_T \frac{\partial^3 v}{\partial x^3} &= 0 \quad \text{zero shear on composite beam}
 \end{aligned}
 \tag{39}$$

Substituting Eqns 37 into Eqns 38 and 39 produces a set of eight simultaneous equations in the eight constants, A_1, \dots, A_6, B_7 and B_8 . In this case, the constants B_7 and B_8 can be eliminated from the system, reducing the number of simultaneous equations to be satisfied to six.

The equations are, in matrix form

$$\begin{bmatrix} 1 & 1 & 1 & 1 & 1 & 1 \\ p_1 & p_2 & p_3 & p_4 & p_5 & p_6 \\ \Psi_1 & \Psi_2 & \Psi_3 & \Psi_4 & \Psi_5 & \Psi_6 \\ \Psi_1 p_1 e^{p_1 L} & \Psi_2 p_2 e^{p_2 L} & \Psi_3 p_3 e^{p_3 L} & \Psi_4 p_4 e^{p_4 L} & \Psi_5 p_5 e^{p_5 L} & \Psi_6 p_6 e^{p_6 L} \\ p_1^2 e^{p_1 L} & p_2^2 e^{p_2 L} & p_3^2 e^{p_3 L} & p_4^2 e^{p_4 L} & p_5^2 e^{p_5 L} & p_6^2 e^{p_6 L} \\ h_1 e^{p_1 L} & h_2 e^{p_2 L} & h_3 e^{p_3 L} & h_4 e^{p_4 L} & h_5 e^{p_5 L} & h_6 e^{p_6 L} \end{bmatrix} \times \begin{pmatrix} A_1 \\ A_2 \\ A_3 \\ A_4 \\ A_5 \\ A_6 \end{pmatrix} = \begin{pmatrix} 0 \\ 0 \\ 0 \\ 0 \\ 0 \\ 0 \end{pmatrix} \quad (40)$$

where

$$\Psi_j = \beta_j - \gamma_j$$

and

$$h_j = d_1(\gamma_j - \beta_j) + d_1^2 t_{v1} p_j - \frac{D_T p_j^3}{G_{v1}}$$

Base Layer Fixed at $x = 0$ and Free at $x = L$; Constraining Layer Free at $x = 0$ and at $x = L$

This is an example of mixed boundary conditions. Comparing this case to the previous one will illustrate the effect of considering mixed boundary conditions on the loss factor. The boundary

conditions are; at $x = 0$

$$\begin{aligned}
 \partial v / \partial x &= 0 \quad \text{zero slope} \\
 v &= 0 \quad \text{zero lateral displacement} \\
 u_{e0} &= 0 \quad \text{zero longitudinal displacement of base layer} \\
 \partial u_{e1} / \partial x &= 0 \quad \text{zero longitudinal force on constraining layer}
 \end{aligned}
 \tag{41}$$

and, at $x = L$

$$\begin{aligned}
 \partial u_{e0} / \partial x &= 0 \quad \text{zero longitudinal force on base layer} \\
 \partial u_{e1} / \partial x &= 0 \quad \text{zero longitudinal force on constraining layer} \\
 \partial^2 v / \partial x^2 &= 0 \quad \text{zero moment on composite beam} \\
 G_{v1} d_1 t & \left[\frac{v - u_{e0}}{t_{v1}} + d_1 \frac{\partial v}{\partial x} \right] - D_T \frac{\partial^3 v}{\partial x^3} \\
 &= 0 \quad \text{zero shear on composite beam}
 \end{aligned}
 \tag{42}$$

Since the boundary conditions on the elastic layers are different at $x = 0$, the constants B_7 and B_8 cannot be eliminated. The equations are, in matrix form

$$\begin{bmatrix} 1 & 1 & 1 & 1 & 1 & 1 & 0 & 0 \\ p_1 & p_2 & p_3 & p_4 & p_5 & p_6 & 0 & 0 \\ \beta_1 & \beta_2 & \beta_3 & \beta_4 & \beta_5 & \beta_6 & 1 & 0 \\ \gamma_1 p_1 & \gamma_2 p_2 & \gamma_3 p_3 & \gamma_4 p_4 & \gamma_5 p_5 & \gamma_6 p_6 & 0 & 1 \\ \beta_1 p_1 e^{p_1 L} & \beta_2 p_2 e^{p_2 L} & \beta_3 p_3 e^{p_3 L} & \beta_4 p_4 e^{p_4 L} & \beta_5 p_5 e^{p_5 L} & \beta_6 p_6 e^{p_6 L} & 0 & 1 \\ \gamma_1 p_1 e^{p_1 L} & \gamma_2 p_2 e^{p_2 L} & \gamma_3 p_3 e^{p_3 L} & \gamma_4 p_4 e^{p_4 L} & \gamma_5 p_5 e^{p_5 L} & \gamma_6 p_6 e^{p_6 L} & 0 & 1 \\ p_1^2 e^{p_1 L} & p_2^2 e^{p_2 L} & p_3^2 e^{p_3 L} & p_4^2 e^{p_4 L} & p_5^2 e^{p_5 L} & p_6^2 e^{p_6 L} & 0 & 0 \\ h_1 e^{p_1 L} & h_2 e^{p_2 L} & h_3 e^{p_3 L} & h_4 e^{p_4 L} & h_5 e^{p_5 L} & h_6 e^{p_6 L} & 0 & 0 \end{bmatrix}$$

$$\times \begin{pmatrix} A_1 \\ A_2 \\ A_3 \\ A_4 \\ A_5 \\ A_6 \\ B_7 \\ B_8 \end{pmatrix} = \begin{pmatrix} 0 \\ 0 \\ 0 \\ 0 \\ 0 \\ 0 \\ 0 \\ 0 \end{pmatrix} \quad (43)$$

Although this cannot be reduced to six simultaneous equations, the sparsity of the last two rows simplifies the calculation of the determinant. It is apparent that, at the most, three six by six determinants need to be calculated.

Base Layer Pinned at $x = 0$ and at $x = L$; Constraining Layer Free at $x = 0$ and Free at $x = L$

This boundary condition was selected for comparison with known solutions. It is closest to the simply supported composite boundary condition which was the first case solved in the literature (8).

The boundary conditions are; at both $x = 0$ and $x = L$

$$\begin{aligned} v &= 0 && \text{zero lateral displacement} \\ \partial^2 v / \partial x^2 &= 0 && \text{zero moment on the composite beam} \\ u_{e0} &= 0 && \text{zero longitudinal displacement of base layer} \\ \partial u_{e1} / \partial x &= 0 && \text{zero longitudinal force on constraining layer} \end{aligned} \tag{44}$$

The equations are

$$\begin{bmatrix} 1 & 1 & 1 & 1 & 1 & 1 & 0 & 0 \\ p_1^2 & p_2^2 & p_3^2 & p_4^2 & p_5^2 & p_6^2 & 0 & 0 \\ \beta_1 & \beta_2 & \beta_3 & \beta_4 & \beta_5 & \beta_6 & 1 & 0 \\ \gamma_1 p_1 & \gamma_2 p_2 & \gamma_3 p_3 & \gamma_4 p_4 & \gamma_5 p_5 & \gamma_6 p_6 & 0 & 1 \\ \beta_1 e^{p_1 L} & \beta_2 e^{p_2 L} & \beta_3 e^{p_3 L} & \beta_4 e^{p_4 L} & \beta_5 e^{p_5 L} & \beta_6 e^{p_6 L} & 1 & L \\ \gamma_1 p_1 e^{p_1 L} & \gamma_2 p_2 e^{p_2 L} & \gamma_3 p_3 e^{p_3 L} & \gamma_4 p_4 e^{p_4 L} & \gamma_5 p_5 e^{p_5 L} & \gamma_6 p_6 e^{p_6 L} & 0 & 1 \\ p_1^2 e^{p_1 L} & p_2^2 e^{p_2 L} & p_3^2 e^{p_3 L} & p_4^2 e^{p_4 L} & p_5^2 e^{p_5 L} & p_6^2 e^{p_6 L} & 0 & 0 \\ e^{p_1 L} & e^{p_2 L} & e^{p_3 L} & e^{p_4 L} & e^{p_5 L} & e^{p_6 L} & 0 & 0 \end{bmatrix}$$

$$\times \begin{pmatrix} A_1 \\ A_2 \\ A_3 \\ A_4 \\ A_5 \\ A_6 \\ B_7 \\ B_8 \end{pmatrix} = \begin{pmatrix} 0 \\ 0 \\ 0 \\ 0 \\ 0 \\ 0 \\ 0 \\ 0 \end{pmatrix} \quad (45)$$

In this case, by subtracting row five from row three, B_7 can be eliminated and the number of simultaneous equations reduced to seven.

Base Layer Pinned at $x = 0$ and at $x = L$; Constraining Layer Rotates with Base Layer at $x = 0$ and Free at $x = L$

This is a variation on the simply supported case in the previous section, and will be used to illustrate the effect of permitting mixed boundary conditions. The constraining layer is 'rigidly

connected' to the base layer at $x = 0$, such that all layers rotate together at that end. The constraining layer will have a non-zero enforced displacement.

At first glance this appears to be a non-homogeneous boundary condition. All the boundary conditions considered so far have been homogeneous, i.e. all zeros appear on the right hand side of the equations. An arbitrary enforced nonzero displacement is a non-homogeneous boundary condition. However, the enforced displacement in this case is not arbitrary, but is related to the slope of the beam. For small rotations, at $x = 0$

$$u_{e1} \approx - \left(\frac{t_{e0} + t_{e1}}{2} + t_{v1} \right) \frac{\partial v}{\partial x} = -t_{v1} d_1 \frac{\partial v}{\partial x} \quad (46)$$

Since $\partial v / \partial x$ contains only terms in $A_1 \dots A_6$, this displacement can be included in the left-hand side of the boundary condition equation, and the boundary condition is seen to be homogeneous.

The boundary conditions are; at $x = 0$

$$\begin{aligned} v &= 0 && \text{zero lateral displacement} \\ \partial^2 v / \partial x^2 &= 0 && \text{zero moment on the composite beam} \\ u_{e0} &= 0 && \text{zero longitudinal displacement of base layer} \\ u_{e1} &= -t_{v1} d_1 (\partial v / \partial x) && \text{constraining layer rotates with the base layer} \end{aligned} \quad (47)$$

and $x = l$

$$\begin{aligned} v &= 0 && \text{zero lateral displacement} \\ \partial^2 v / \partial x^2 &= 0 && \text{zero moment on the composite beam} \\ u_{e0} &= 0 && \text{zero longitudinal displacement of base layer} \\ \partial u_{e1} / \partial x &= 0 && \text{zero longitudinal force on constraining layer} \end{aligned} \quad (48)$$

The matrix equation is

$$\begin{bmatrix} 1 & 1 & 1 & 1 & 1 & 1 & 0 & 0 \\ p_1^2 & p_2^2 & p_3^2 & p_4^2 & p_5^2 & p_6^2 & 0 & 0 \\ \beta_1 & \beta_2 & \beta_3 & \beta_4 & \beta_5 & \beta_6 & 1 & 0 \\ \Gamma_1 & \Gamma_2 & \Gamma_3 & \Gamma_4 & \Gamma_5 & \Gamma_6 & 1 & 0 \\ \beta_1 e^{p_1 L} & \beta_2 e^{p_2 L} & \beta_3 e^{p_3 L} & \beta_4 e^{p_4 L} & \beta_5 e^{p_5 L} & \beta_6 e^{p_6 L} & 1 & L \\ \gamma_1 p_1 e^{p_1 L} & \gamma_2 p_2 e^{p_2 L} & \gamma_3 p_3 e^{p_3 L} & \gamma_4 p_4 e^{p_4 L} & \gamma_5 p_5 e^{p_5 L} & \gamma_6 p_6 e^{p_6 L} & 0 & 1 \\ p_1^2 e^{p_1 L} & p_2^2 e^{p_2 L} & p_3^2 e^{p_3 L} & p_4^2 e^{p_4 L} & p_5^2 e^{p_5 L} & p_6^2 e^{p_6 L} & 0 & 0 \\ e^{p_1 L} & e^{p_2 L} & e^{p_3 L} & e^{p_4 L} & e^{p_5 L} & e^{p_6 L} & 0 & 0 \end{bmatrix}$$

$$\times \begin{pmatrix} A_1 \\ A_2 \\ A_3 \\ A_4 \\ A_5 \\ A_6 \\ B_7 \\ B_8 \end{pmatrix} = \begin{pmatrix} 0 \\ 0 \\ 0 \\ 0 \\ 0 \\ 0 \\ 0 \\ 0 \end{pmatrix} \quad (49)$$

where

$$\Gamma_j = \gamma_j + t_{01} d_1 p_j$$

Neither B_7 nor B_8 can be eliminated in this case.

In Chapter VII, numerical results are given for the boundary conditions which have been shown here.

VII. Numerical Results

The equations presented in the previous chapters were programmed and results calculated for some example cases. The name of the program used in the calculations is 'BEAM'. The cases considered were intended to do two things: validate the equations and software, and illustrate the effects of considering mixed boundary conditions.

The first set of cases verify that the equations are valid and the software is working correctly. This is done by demonstrating that the solutions degenerate into known solutions in special cases. The validity of the equations and software are seen in the numerical results, as well as in the mode shapes predicted by BEAM. It will be shown that the software performs as expected.

The second set of test cases demonstrate the effect of permitting mixed boundary conditions, and show how the computed results compare with previously published approximate methods.

For input data, all cases use some variation of the physical parameters in an example calculation in a design guide published in 1985 (16:5-26). This was done to permit comparison with the results in the design guide. The data is shown in Table 2. The physical properties of the viscoelastic material come from the third volume of the design guide, reference (17:263-270).

Computer Programming Approach

Computer software was written to implement the equations shown in the previous sections. The main program is called BEAM. In this section the programming approach is discussed. The numerical techniques are explained briefly. A detailed description of input data is included as Appendix B. Programming notes are in Appendix C. Appendix C also describes the computer and compiler used, data availability, etc.

As pointed out by Rao (13), solving the equations for boundary conditions other than simply supported presents some numerical difficulty. The boundary condition matrix tends to be ill-conditioned (4:175). This can be attributed primarily to the exponential terms. The roots of

Table 2. Basic Data Used as Starting Point for All Test Cases (16:5-26) (17:263-270)

1. Base Layer, aluminum
2. Adhesive Layer, SoundCoat DIAD no. 606
3. Constraining Layer, aluminum

Variable	Value	Units
L	0.254	meter
E_{e0}	$6.8900e10$	Pascal
t_{e0}	$5.0800e-3$	meter
ρ_{e0}	$2.7700e 3$	(kg)/meter ³
ν_{e0}	0.3300	
t_{v1}	$2.5400e-4$	meter
ρ_{v1}	$9.6900e 2$	(kg)/meter ³
E_{e1}	$6.8900e10$	Pascal
t_{e1}	$2.5400e-4$	meter
ρ_{e1}	1.0	(kg)/meter ³
ν_{e1}	0.3300	
A(1)	335.0	degrees K
A(2)	280.0	degrees K
A(3)	390.0	degrees K
A(4)	$0.7e-1$	degrees K/Hz
A(5)	0.1142	degrees K/Hz
A(6)	$0.3e-1$	degrees K/Hz
B(1)	$0.2e6$	Pascal
B(2)	$1200.0e6$	Pascal
B(3)	$0.3e7$	Hz
B(4)	0.55	
B(5)	1.5	
B(6)	0.1	

the characteristic equation come in pairs. Even modest values of p_j produce both very large and very small terms in the matrix. In BEAM, two things are done to ensure accurate calculation of the determinant. First, double precision arithmetic is used in all calculations. Second, total pivoting is used in the gaussian elimination algorithm, rather than scaled partial pivoting (4:159). The determinant is calculated using triangular factorization (4:160). Triangular factorization is a gaussian elimination algorithm. Rows and/or columns are exchanged during the elimination to reduce round-off error. In scaled partial pivoting, only rows are interchanged. In total pivoting, both rows and columns are interchanged as necessary. Total pivoting is slower than scaled partial pivoting because it involves more overhead. It is also more complicated because the program must keep track of both row and column interchanges. For these reasons, total pivoting is seldom used. In this case, total pivoting was necessary to ensure accuracy.

While it would clearly be possible to locate zeros of the determinant using a root finding algorithm such as Muller's method (4:120), there are disadvantages to using this approach. Most root finders (4:72-127) assume prior knowledge of approximate locations of zeros, and they may not converge if they are not in the vicinity of a zero. Also, they cannot be expected to find all zeros. The magnitude of the boundary condition determinant tends to increase as ω increases, so if good initial estimates are not available a root finder is not likely to converge to a root.

In BEAM, zeros were located using a simple grid search rather than a more complex root finding algorithm. The grid search is described below. A more efficient routine should be implemented in practice, but for the purposes of investigating the locations of the minima, the grid search was very useful, and it avoided potential convergence problems. The grid search is not fast, but it is robust and dependable. It is more practical than it is elegant.

In the grid search, the user specifies a range of values for real and imaginary frequency, and an increment for both real and imaginary values. The software calculates values for the magnitude of the determinant at every value of real and imaginary frequency specified. This is the grid. The

software then checks all points on the grid for relative minima. If a minimum is found, the grid is refined in the vicinity of the minimum to improve the accuracy. The surface defined by the magnitude of the boundary condition determinant is relatively smooth, making it easy to locate minima. If the initial grid is fine enough, the grid search will find all minima in a given range.

After the minima are found, it then remains to determine which are actually solutions which satisfy the boundary conditions, i.e. which are 'zeros'. There are several ways to validate a zero. First, the value is substituted back into the boundary condition equations. If the error in a boundary condition equation is roughly the same order of magnitude of the individual terms of the equation, then that boundary condition is not satisfied (4:169-176). If the error in a boundary condition is small compared to the individual terms, then the equation is satisfied. Zeros can also be verified by solving for A_j , p_j , B_7 and B_8 , β_j and γ_j at that value of frequency, then using these terms to calculate a mode shape. The mode shapes show clearly whether the boundary condition has been satisfied. Zeros can also be identified by comparison with previously found zeros. The actual solutions tend to lie on a smooth curve. Any minima which lie well outside the trend are not likely to satisfy the boundary conditions.

Test Cases for Validating Software

Three test cases were considered for which comparisons could be made with theoretical results. The first two cases were for a cantilever beam with the constraining layer fixed at $x = 0$. This is the first boundary condition listed in Table 1. These two cases used input data for the layered beam for which the frequencies could be expected to approach the frequencies of an undamped cantilever beam. The third uses the third boundary condition in Table 1, and the input data in Table 2. This boundary condition should closely resemble the simply supported case in the literature.

Case 1 - Bare Beam The first test case approximated a bare cantilever beam, by letting the shear modulus of the damping layer be small, and the elastic modulus and density of the

Table 3. Data Used to Calculate Theoretical Frequencies for Cases 1 and 2

Variable	Case 1	Case 2	Units
E	6.8900e10	6.8900e10	Pascal
I	1.0925e-8	1.2990e-8	meter ⁴
L	0.254	0.254	meter
m/L	14.0716	15.0213	(kg)/meter

constraining layer be small. The problem formulation does not permit the numbers to be set to exactly zero. In some cases, setting a value to zero would result in division by zero. In other cases it would cause excessive roundoff errors. Trial and error was used to find the smallest values the software would accept. The real part of the resulting complex frequencies which satisfy the boundary conditions should approach the natural frequencies of a simple cantilever beam. The imaginary part of the complex frequencies should approach zero, corresponding to zero damping.

The theoretical natural frequencies are roots to the transcendental equation (10:224-227)

$$\cos \lambda L \cosh \lambda L = -1 \quad (50)$$

where

$$\lambda^4 = \frac{\omega^2 m}{EI}$$

Table 3 lists the data used to calculate the theoretical frequencies, and Table 4 lists the input data for calculating the natural frequencies in BEAM. Data not listed in Table 4 was unchanged from that shown in Table 2. Note that, in this case, the shear modulus, G_{v1} , was held constant for all frequencies, rather than letting it vary according to Eqns 6 and 7. Table 5 lists the resulting natural frequencies for the first six modes as predicted by Eqn 50, and the complex frequencies predicted by BEAM.

Note in Table 5 that the imaginary frequencies predicted by BEAM are zero or very small, suggesting small damping, as expected. All real frequencies are 5.9% high. This could be the result of letting the parameters of the top layers be small, but not zero.

Table 4. Input Data for Program BEAM for Cases 1 and 2

Variable	Bare Beam	Rigid Spacer	Units
	Case 1	Case 2	
G_{v1}	$1.0000 + 1.0i$	$3.0000e 9 + 1.0i$	Pascal
ρ_{v1}	1.0000	1.0000	(kg)/meter ³
E_{e1}	$1.0000e 4 + 0.0i$	$6.8900e10 + 0.0i$	Pascal
t_{e1}	$2.5400e-4$	$2.5400e-4$	meter
ρ_{e1}	1.0	$2.7700e 3$	(kg)/meter ³

Table 5. Case 1 - Comparison of Bare Beam Theoretical Frequencies with Values Predicted by BEAM

Frequencies are in radians/second

Mode	Expected	BEAM		error in Real freq
		Real	Imag	
1	398.59	422.23	0.0000	5.9 %
2	2497.92	2646.10	0.0000	5.9 %
3	6994.25	7409.17	0.0000	5.9 %
4	13705.93	14519.03	0.0000	5.9 %
5	22656.89	24000.99	0.0001	5.9 %
6	33854.47	35853.33	0.0001	5.9 %

Case 2 - Rigid Spacer Case 2 approximates an undamped beam with a rigid spacer. In BEAM, the real part of the shear modulus of the viscoelastic layer was made large, and the imaginary part small. As in case 1, the theoretical natural frequencies of the beam were found by solving Eqn 50. A beam with a rigid spacer will have a slightly larger moment of inertia than a bare beam, due to the separation between the two elastic layers. The mass per unit length will be larger than the bare beam because of the addition of the mass of the constraining layer. The data used to calculate the theoretical natural frequencies for this case is shown in Table 3. The input data used in program BEAM for case 2 is shown in Table 4. As in the first case, the complex shear modulus is not permitted to vary with frequency according to Eqns 6 and 7, but remains fixed. The theoretical natural frequencies, and the complex frequencies predicted by BEAM, are listed in Table 6.

Again, the imaginary components of the frequency are zero, as expected. The real components are all slightly high.

Table 6. Case 2 - Comparison of Rigid Spacer Theoretical Frequencies with Values Predicted by BEAM

Mode	Expected	BEAM		error in Real freq
		Real	Imag	
1	420.67	445.42	0.0000	5.9%
2	2636.31	2791.29	0.0000	5.9%
3	7381.75	7815.16	0.0000	5.9%
4	14465.29	15313.04	0.0000	5.9%
5	23912.16	25310.22	0.0000	5.9%
6	35720.63	37803.00	0.0000	5.9%

It should be noted that the derivation of Eqn 50 assumes that shear strain energy is negligible (10:221). Permitting the layered beam to have a rigid spacer, i.e. very high shear modulus, could intuitively be expected to result in higher natural frequencies than the bare beam.

Case 3 - Simply Supported Historically, the first boundary condition solved for the layered beam was the simply supported case (8). The solution is of the form

$$v = D \sin \left(\frac{n\pi x}{L} \right) \quad (51)$$

where

- D = a constant
- n = the mode number
- π = 3.14159 ...
- x = distance along the length of the beam
- L = the length of the beam

Although the literature does not address the longitudinal displacement of the elastic layers, intuitively one would expect the displacement of the constraining layer to have the form

$$u_{e1} = F \cos \left(\frac{n\pi x}{L} \right) \quad (52)$$

where

$$F = \text{a constant}$$

This can be justified with a simple argument. When the composite beam is deflected upward in the center, the longitudinal displacement of the top layer should be zero in the center. It should also be some negative value at $x = 0$ and the same positive value at $x = L$.

It is not immediately apparent what form the longitudinal deflection of the base layer would take, since it is restrained at both ends.

In this section, it will be demonstrated that the BEAM results satisfy Eqns 51 and 52 when the base layer is simply supported and the top layer is completely unrestrained.

Taking the real part of the expressions for v and u_{e1} in Eqns 25 results in, for a given p ,

$$\text{Re}(v) = e^{p_R x} [A_R \cos(p_I x) - A_I \sin(p_I x)] \quad (53)$$

and

$$\text{Re}(u_{e1}) = e^{p_R x} [(\gamma_R A_R - \gamma_I A_I) \cos(p_I x) - (\gamma_R A_I + \gamma_I A_R) \sin(p_I x)] \quad (54)$$

The subscript R denotes the real part and the subscript I denotes the imaginary part of a quantity. Several conditions must be satisfied for Eqns 53 and 54 to reduce to the form of Eqns 51 and 52. The p_j come in pairs, and they are eigenvalues of the system, so there should be exactly one pair of p_j such that

$$p_R = 0 \quad \text{and} \quad p_I = \pm \frac{n\pi}{L} \quad (55)$$

If the pair of roots which meet the condition of Eqn 55 are arbitrarily designated p_1 and p_2 , it can be shown that the coefficients $A_1 \dots A_6$ and $\gamma_1 \dots \gamma_6$ must satisfy the following conditions:

$$\begin{aligned}
 A_{1,R} + A_{2,R} &= 0 \\
 A_{1,I} - A_{2,I} &\neq 0 \\
 A_{3,R} + A_{4,R} &= 0 \\
 A_{3,I} - A_{4,I} &= 0 \\
 A_{5,R} + A_{6,R} &= 0 \\
 A_{5,I} - A_{6,I} &= 0
 \end{aligned} \tag{56}$$

$$\begin{aligned}
 (\gamma_{1,R}A_{1,R} - \gamma_{1,I}A_{1,I}) + (\gamma_{2,R}A_{2,R} - \gamma_{2,I}A_{2,I}) &\neq 0 \\
 (\gamma_{1,R}A_{1,I} - \gamma_{1,I}A_{1,R}) - (\gamma_{2,R}A_{2,I} - \gamma_{2,I}A_{2,R}) &= 0 \\
 (\gamma_{3,R}A_{3,R} - \gamma_{3,I}A_{3,I}) + (\gamma_{4,R}A_{4,R} - \gamma_{4,I}A_{4,I}) &= 0 \\
 (\gamma_{3,R}A_{3,I} - \gamma_{3,I}A_{3,R}) - (\gamma_{4,R}A_{4,I} - \gamma_{4,I}A_{4,R}) &= 0 \\
 (\gamma_{5,R}A_{5,R} - \gamma_{5,I}A_{5,I}) + (\gamma_{6,R}A_{6,R} - \gamma_{6,I}A_{6,I}) &= 0 \\
 (\gamma_{5,R}A_{5,I} - \gamma_{5,I}A_{5,R}) - (\gamma_{6,R}A_{6,I} - \gamma_{6,I}A_{6,R}) &= 0
 \end{aligned} \tag{57}$$

If the conditions in Eqns 56 are satisfied, only a sine term will remain in the expression for v . Similarly, if the conditions in Eqns 57 are satisfied, only a cosine term will remain in the expression for u_{e1} .

Note that the subscripts in Eqns 55 ... 57 are arbitrary. The only requirement is that the nonzero terms in Eqns 56 and 57 must be associated with the two p_j which satisfy Eqns 55. Any two, but only two, p_j are expected to satisfy Eqns 55. In the numerical results, simply as a consequence of the way the software was written, these roots will have 'adjacent' indices. In other words, they could be satisfied by p_1 and p_2 , by p_3 and p_4 , or by p_5 and p_6 . In Eqns 56 and 57 the nonzero terms would have the same subscripts as the pair of p_j which satisfy Eqns 55.

Table 7. BEAM Output, Test Case 3, Mode 1

At Omega = 1221.86 +14.46i Radians per second:							
P		Beta		Gamma			
J	Real	Imag	Real	Imag	Real	Imag	
1	21.15	8.49	-.1667E-01	-.8685E-02	0.3334E+00	0.1737E+00	
2	-21.15	-8.49	0.1667E-01	0.8685E-02	-.3334E+00	-.1737E+00	
3	0.00	-12.38	0.2589E-03	-.1332E-02	-.5178E-02	0.2664E-01	
4	0.00	12.38	-.2589E-03	0.1332E-02	0.5178E-02	-.2664E-01	
5	12.18	.23	0.2075E-02	-.5778E-03	-.4149E-01	0.1156E-01	
6	-12.18	-.23	-.2075E-02	0.5778E-03	0.4149E-01	-.1156E-01	
Constants A...							
J	Real		Imag				
1	0.69418126E-05		0.00000000E+00				
2	-.82489694E-03		0.12445740E-02				
3	0.25344642E+00		0.65964374E+00				
4	-.25552087E+00		-.65962757E+00				
5	0.12232727E-03		-.61542895E-04				
6	0.27700760E-02		-.11991999E-02				
7	-.18594580E-02		0.31897464E-03				
8	0.14641401E-01		-.25116113E-02				

It now remains to demonstrate that the numerical results from BEAM satisfy the conditions specified. In the test case, the input data listed in Table 2 was used. The shear modulus of the adhesive layer was permitted to vary according to Eqns 6 and 7.

For the first mode, using the input data in Table 2, the requirement on p_I is

$$p_I = \frac{\pi}{L} = \frac{\pi}{0.254} \approx 12.37$$

The output of BEAM for the first mode is shown in Table 7. Table 8 shows the values of the quantities defined by Eqns 56 and 57. In the program output shown in Table 7, the constants B_7 and B_8 are shown as the seventh and eighth values in the vector A . This was done for convenience in programming.

In Table 7, p_3 and p_4 satisfy Eqns 55. Of the terms defined by Eqn 56, the 'nonzero' term is three orders of magnitude larger than the 'zero' terms. Of the terms defined by Eqn 57, the

Table 8. Conditions on Constants A and γ - Case 3 Mode 1

$$\begin{aligned}
 A_{1,R} + A_{2,R} &= -8.1796E - 04 \\
 A_{1,I} - A_{2,I} &= -1.2446E - 03 \\
 A_{3,R} + A_{4,R} &= -2.0744E - 03 \\
 A_{3,I} - A_{4,I} &= +1.3190 \\
 A_{5,R} + A_{6,R} &= +2.8924E - 03 \\
 A_{5,I} - A_{6,I} &= +1.1377E - 03
 \end{aligned}$$

$$\begin{aligned}
 (\gamma_{1,R}A_{1,R} - \gamma_{1,I}A_{1,I}) + (\gamma_{2,R}A_{2,R} - \gamma_{2,I}A_{2,I}) &= +4.9347E - 04 \\
 (\gamma_{1,R}A_{1,I} - \gamma_{1,I}A_{1,R}) - (\gamma_{2,R}A_{2,I} - \gamma_{2,I}A_{2,R}) &= +5.5696E - 04 \\
 (\gamma_{3,R}A_{3,R} - \gamma_{3,I}A_{3,I}) + (\gamma_{4,R}A_{4,R} - \gamma_{4,I}A_{4,I}) &= -3.7779E - 02 \\
 (\gamma_{3,R}A_{3,I} - \gamma_{3,I}A_{3,R}) - (\gamma_{4,R}A_{4,I} - \gamma_{4,I}A_{4,R}) &= +5.5178E - 05 \\
 (\gamma_{5,R}A_{5,R} - \gamma_{5,I}A_{5,I}) + (\gamma_{6,R}A_{6,R} - \gamma_{6,I}A_{6,I}) &= +9.6719E - 05 \\
 (\gamma_{5,R}A_{5,I} - \gamma_{5,I}A_{5,R}) - (\gamma_{6,R}A_{6,I} - \gamma_{6,I}A_{6,R}) &= +1.8887E - 05
 \end{aligned}$$

'nonzero' term is two orders of magnitude larger than the 'zero' terms. While this difference in magnitude is technically large enough to meet the requirement, it is not clearly convincing.

The data for the second mode is much better. It is shown in Tables 9 and 10. For the second mode the requirement on p_I is

$$p_I = \frac{2\pi}{L} = \frac{2\pi}{0.254} \approx 24.74$$

In Table 9 it can be seen that p_5 and p_6 satisfy the specified conditions. In Table 10, the constants associated with p_5 and p_6 satisfy Eqns 56 and 57.

The difference in the quality of the calculated results between the first and second modes may be due to the accuracy with which the frequencies were located. Both sets of data were calculated in the same run, using the same tolerance. The software uses several tolerances to decide how closely to refine the accuracy of a frequency. The magnitude of the determinant, or the change in magnitude of the determinant from one iteration to the next, or the difference in frequencies from one iteration to the next, are all criteria which could terminate the search. These are explained in more detail in Appendix B. One of these criteria may have been satisfied with a less accurate calculation of the first frequency than the second. Still, for both modes, it is safe to say that the BEAM results degenerate into the theoretical solutions shown in Eqns 51 and 52.

Table 9. BEAM Output, Test Case 3, Mode 2

At Omega =	4820.67	+75.75i Radians per second:				
	P	Beta		Gamma		
J	Real	Imag	Real	Imag	Real	Imag
1	29.95	12.00	-.2025E-01	-.1904E-01	0.4049E+00	0.3808E+00
2	-29.95	-12.00	0.2025E-01	0.1904E-01	-.4049E+00	-.3808E+00
3	24.19	1.00	0.3957E-02	-.3047E-02	-.7913E-01	0.6094E-01
4	-24.19	-1.00	-.3957E-02	0.3047E-02	0.7913E-01	-.6094E-01
5	0.00	-24.74	0.7089E-03	-.2110E-02	-.1418E-01	0.4221E-01
6	0.00	24.74	-.7089E-03	0.2110E-02	0.1418E-01	-.4221E-01
Constants A...						
J	Real		Imag			
1	0.80797525E-16		0.00000000E+00			
2	-.86216012E-11		0.21418468E-10			
3	0.13165025E-14		0.54727301E-15			
4	-.11847728E-09		-.18512119E-09			
5	0.57231485E+00		-.41527191E+00			
6	-.57231485E+00		0.41527191E+00			
7	0.94137268E-03		0.30044278E-02			
8	0.17361570E-11		0.25122977E-11			

Table 10. Conditions on Constants A and γ - Case 3 Mode 2

$$\begin{aligned}
 A_{1,R} + A_{2,R} &= -8.6215E - 12 \\
 A_{1,I} - A_{2,I} &= -2.1418E - 11 \\
 A_{3,R} + A_{4,R} &= -1.1848E - 10 \\
 A_{3,I} - A_{4,I} &= +1.8512E - 10 \\
 A_{5,R} + A_{6,R} &= -1.3428E - 10 \\
 A_{5,I} - A_{6,I} &= -0.8305
 \end{aligned}$$

$$\begin{aligned}
 (\gamma_{1,R}A_{1,R} - \gamma_{1,I}A_{1,I}) + (\gamma_{2,R}A_{2,R} - \gamma_{2,I}A_{2,I}) &= +1.1646E - 11 \\
 (\gamma_{1,R}A_{1,I} - \gamma_{1,I}A_{1,R}) - (\gamma_{2,R}A_{2,I} - \gamma_{2,I}A_{2,R}) &= +1.1955E - 11 \\
 (\gamma_{3,R}A_{3,R} - \gamma_{3,I}A_{3,I}) + (\gamma_{4,R}A_{4,R} - \gamma_{4,I}A_{4,I}) &= -2.0656E - 11 \\
 (\gamma_{3,R}A_{3,I} - \gamma_{3,I}A_{3,R}) - (\gamma_{4,R}A_{4,I} - \gamma_{4,I}A_{4,R}) &= +2.1869E - 11 \\
 (\gamma_{5,R}A_{5,R} - \gamma_{5,I}A_{5,I}) + (\gamma_{6,R}A_{6,R} - \gamma_{6,I}A_{6,I}) &= +1.8827E - 02 \\
 (\gamma_{5,R}A_{5,I} - \gamma_{5,I}A_{5,R}) - (\gamma_{6,R}A_{6,I} - \gamma_{6,I}A_{6,R}) &= +8.0772E - 12
 \end{aligned}$$

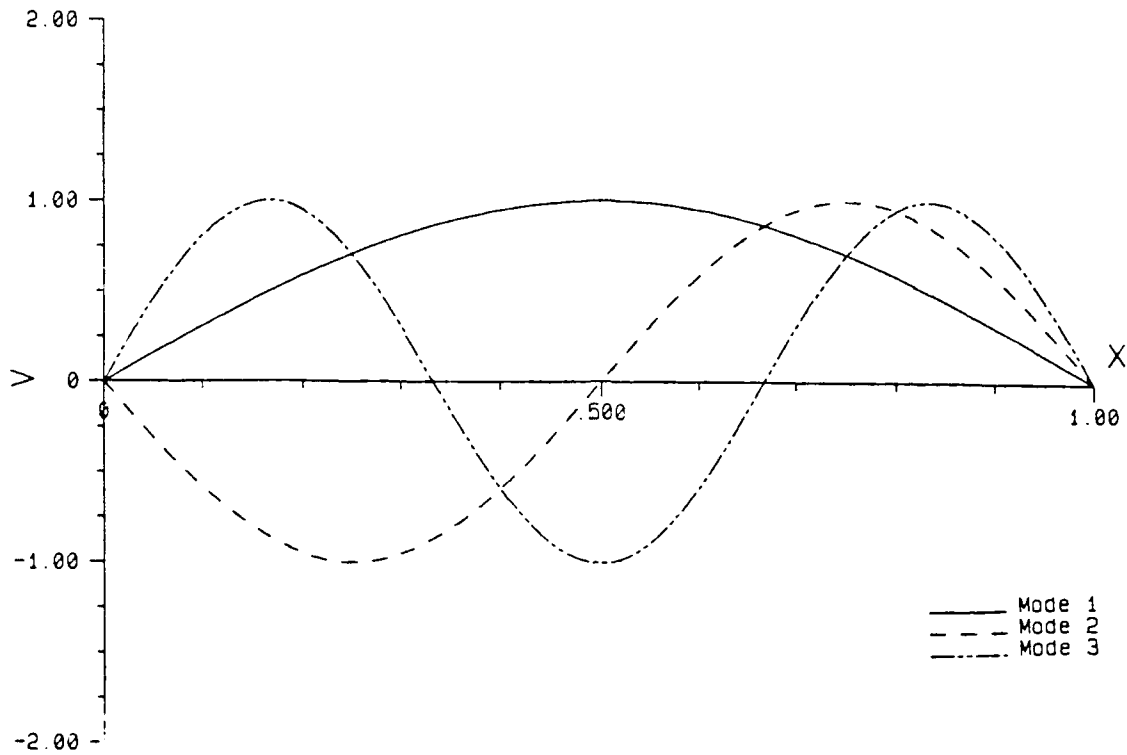


Figure 2. Normalized Lateral Displacement - Base Layer Pinned-Pinned, Constraining Layer Free-Free

The validity of the BEAM results can also be demonstrated by looking at the predicted mode shapes. The mode shapes are calculated by substituting the values of p_j , A_j , β_j , γ_j , B_7 and B_5 into Eqns 37 (without the $e^{i\omega t}$ term). Values of displacement are calculated and plotted for representative values of x . Note that, of the eight constants, one is still unspecified. This can be selected arbitrarily, and is usually used to normalize the mode shapes. The mode shapes still accurately reflect the relative magnitudes of v , u_{e0} and u_{e1} . Figures 2, 3, and 4 show the first three mode shapes for the data presented in this section. The mode shapes are normalized with respect to maximum lateral displacement. That is, the maximum lateral displacement in Figure 2 is set = 1, and the displacements u_{e0} and u_{e1} are adjusted accordingly. The mode shapes are consistent with the stated boundary conditions.

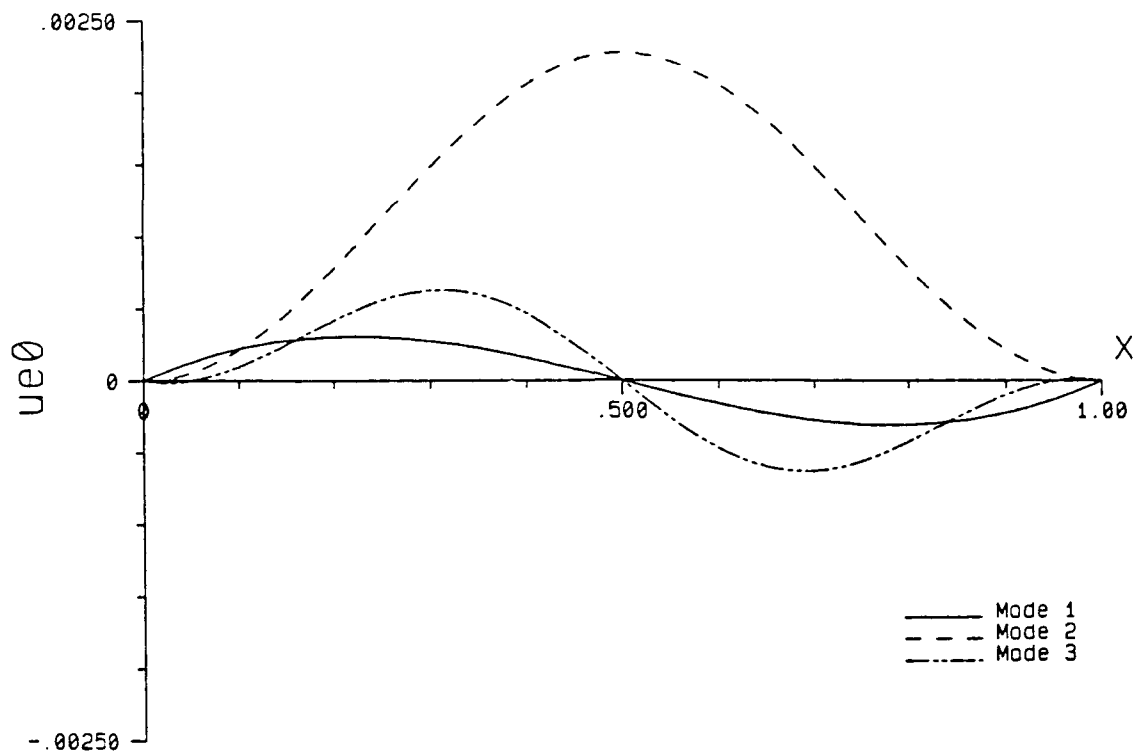


Figure 3. Normalized Longitudinal Displacement of Base Layer - Base Layer Pinned-Pinned, Constraining Layer Free-Free

Test Cases Illustrating the Effect of Considering Mixed Boundary Conditions

In this section, boundary conditions listed in Table 1 are contrasted, to illustrate the effects of considering mixed boundary conditions. Numerical results are also compared to predictions of PREDY, a program published in a damping design guide (16:5-29). PREDY uses approximate formulae to estimate the complex frequencies of a three layer cantilever beam.

Comparison of Complex Frequencies for Cantilever Boundary Conditions This case compares the first and second boundary conditions listed in Table 1, which will be called the cantilever boundary conditions, with results predicted by PREDY (16:5-29). The complex frequencies and loss factors predicted by both BEAM and PREDY are shown, as are mode shapes predicted by BEAM.

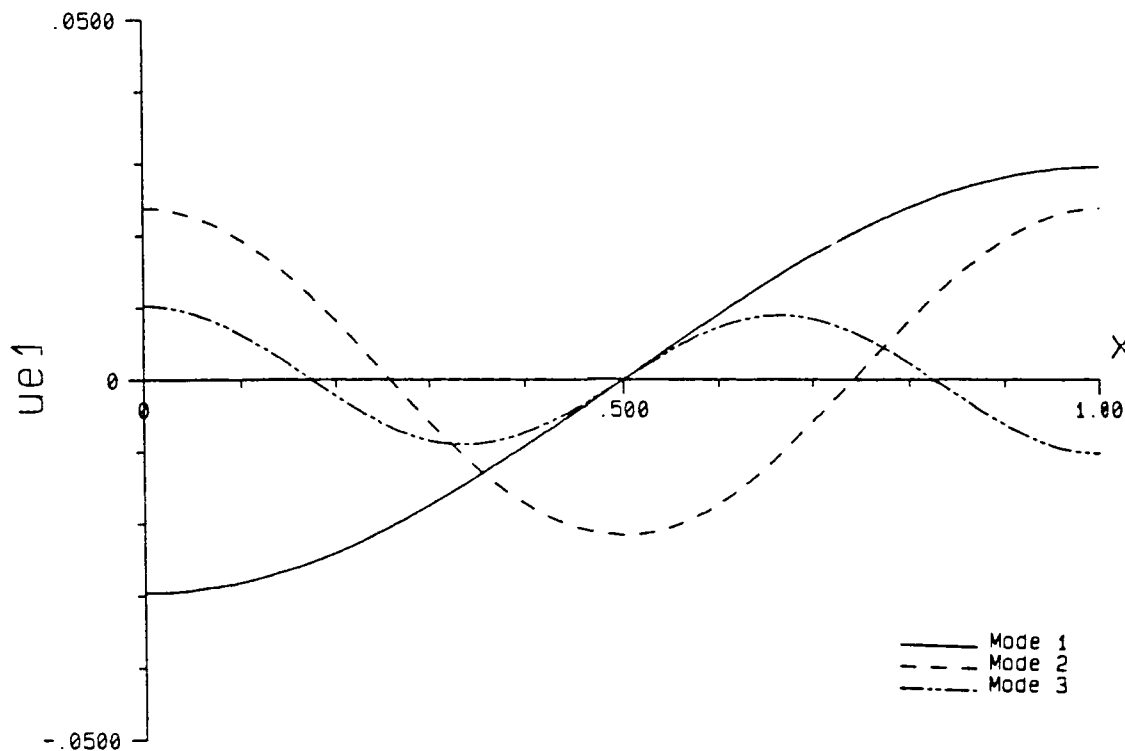


Figure 4. Normalized Longitudinal Displacement of Constraining Layer - Base Layer Pinned-Pinned, Constraining Layer Free-Free

Complex frequencies were calculated using the input data in Table 2 exactly as shown. BEAM calculates real and imaginary frequency components, and PREDY calculates real frequency and loss factor. The quantities are related, as shown in Eqn 12. Intuitively, one would expect the damping to be higher when the constraining layer is fixed, because shear strains are higher.

The complex frequencies predicted by both BEAM and PREDY are shown graphically in Figure 5. Table 11 shows the numerical data used in Figure 5. The complex frequencies for the two cases predicted by BEAM are quite close, while the PREDY calculations tend to predict lower imaginary frequencies in the higher modes. All three calculations show different beam loss factors. It is interesting that all three cases show the maximum loss factor at a different mode. PREDY predicts maximum damping in the second mode, while BEAM predicts maximum damping for the fourth and fifth modes when the constraining layer is fixed-free and free-free, respectively. Except for the first mode, fixing the constraining layer at $x = 0$ results in higher damping, as expected.

Table 11. Values of Complex Frequency Predicted by BEAM and PREDY for Cantilever Boundary Conditions

Mode	BEAM						PREDY		
	Const. Layer Fixed-Free			Const. Layer Free-Free			Real	Imag	η_b
	Real	Imag	η_b	Real	Imag	η_b			
1	437.14	2.78	0.0127	421.02	4.17	0.0198	410.48	4.17	0.0203
2	2697.53	36.32	0.0269	2678.24	25.19	0.0188	2511.78	40.46	0.0322
3	7495.15	114.71	0.0306	7474.49	96.74	0.0259	6946.62	105.29	0.0303
4	14588.14	234.25	0.0321	14570.69	212.39	0.0292	13525.28	180.31	0.0267
5	23990.36	381.06	0.0318	23976.29	358.02	0.0299	22271.59	260.66	0.0234
6	35692.67	547.31	0.0307	35681.46	524.36	0.0294	33184.20	344.23	0.0207

Table 12. Complex Frequencies Predicted by BEAM for Simply Supported Boundary Conditions

Mode	Const. Layer Rigid-Free			Const. Layer Free-Free		
	Real	Imag	η_b	Real	Imag	η_b
1	1199.22	14.07	0.0235	1221.86	14.46	0.0237
2	4780.24	66.14	0.0277	4820.67	75.75	0.0314
3	10704.32	161.38	0.0302	10753.82	182.75	0.0340
4	18942.83	288.94	0.0305	18996.25	319.32	0.0336
5	29488.11	440.83	0.0299	29542.05	478.50	0.0324
6	42331.97	608.42	0.0287	42385.70	651.11	0.0307

The loss factors for the first mode are counter-intuitive, but not unreasonable. The damping is a result primarily of shear strain in the adhesive layer, and the shear strain is related to the difference in longitudinal displacement of the elastic layers, $u_{e0} - u_{e1}$. When both elastic layers are fixed at $x = 0$, the shear strain at that end is zero.

The mode shapes predicted by BEAM for the two cantilever boundary conditions for this example are shown in Figures 6 through 11.

Comparison of Complex Frequencies for Simply Supported Boundary Conditions In this section, the complex frequencies are shown for the two simply supported boundary conditions, which are the third and fourth in Table 1. Again, intuitively, one would expect the loss factor to be higher for the case where the constraining layer is fixed at one end, due to higher shear strains. The locations of the complex frequencies are shown in Figure 12. The data used in Figure 12 is listed in Table 12.

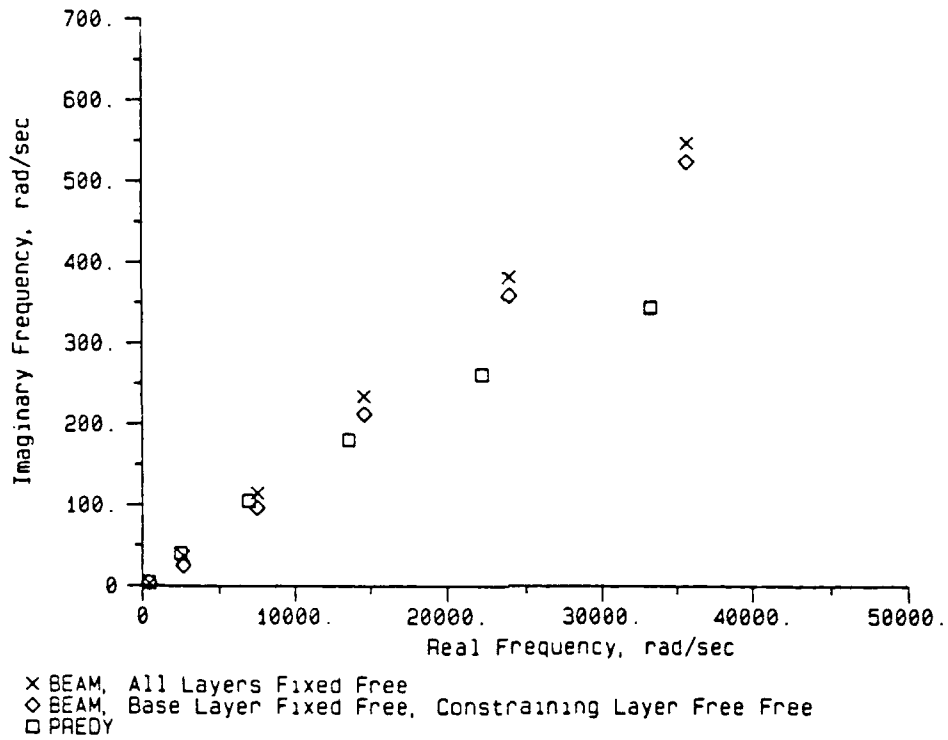


Figure 5. Complex Frequencies for Cantilever Boundary Conditions

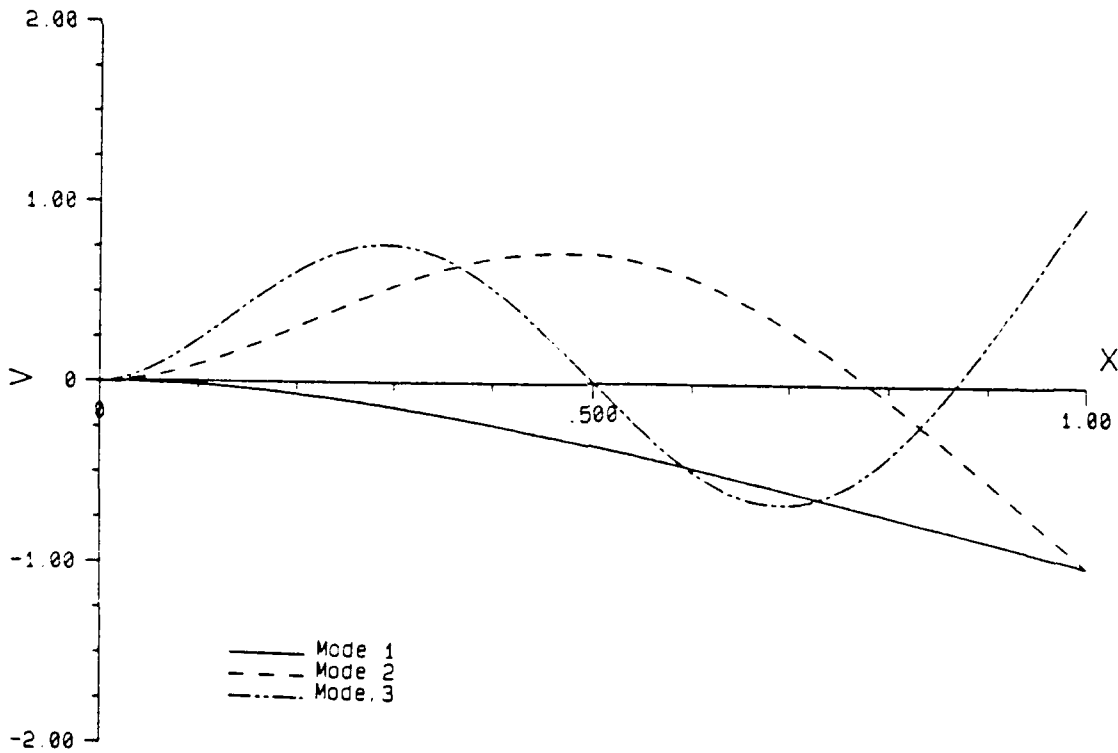


Figure 6. Normalized Lateral Displacement, All Layers Fixed-Free

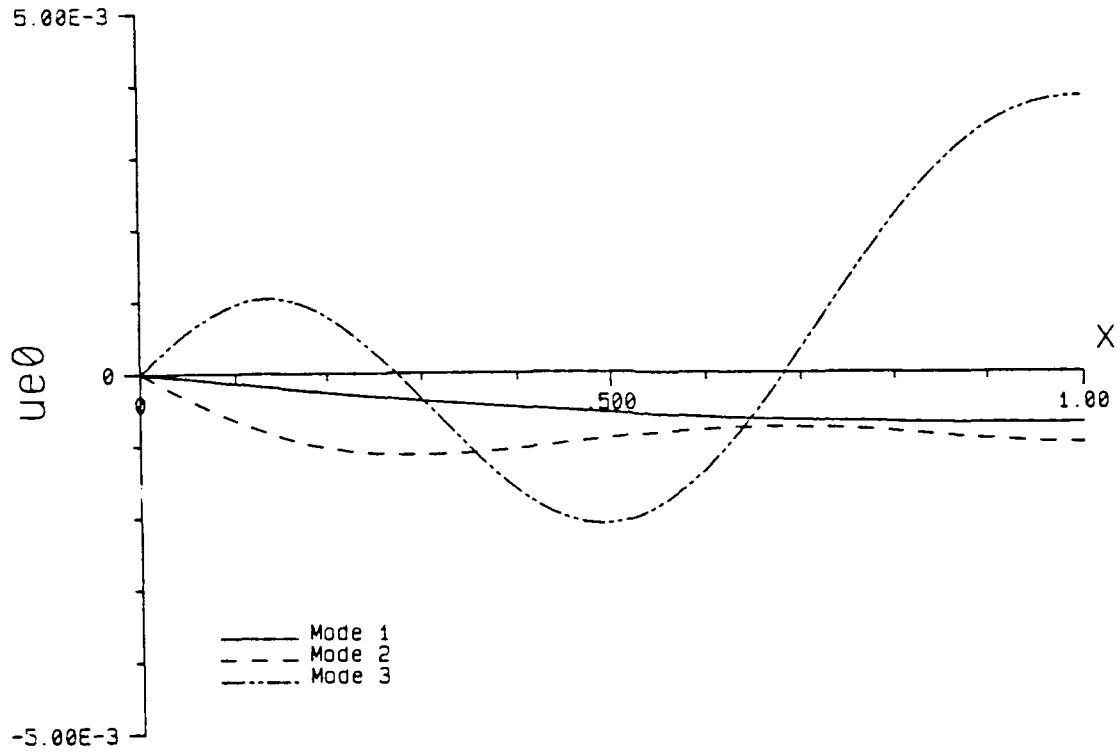


Figure 7. Normalized Longitudinal Displacement of Base Layer, All Layers Fixed-Free

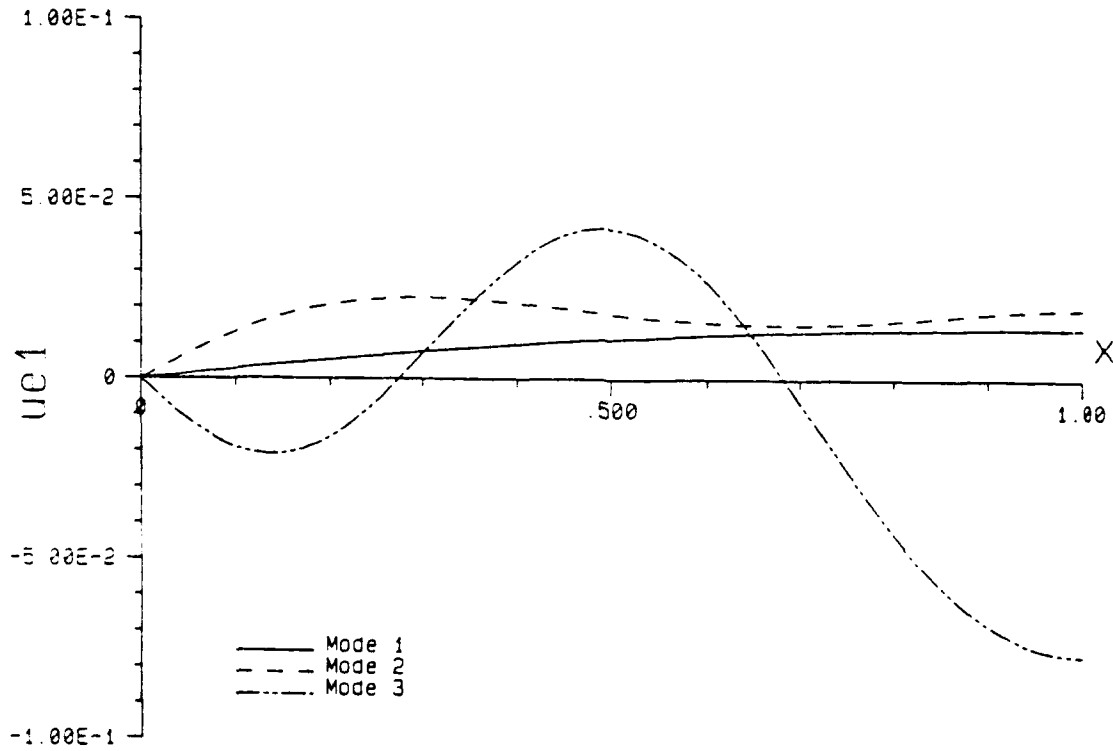


Figure 8. Normalized Longitudinal Displacement of Constraining Layer, All Layers Fixed-Free

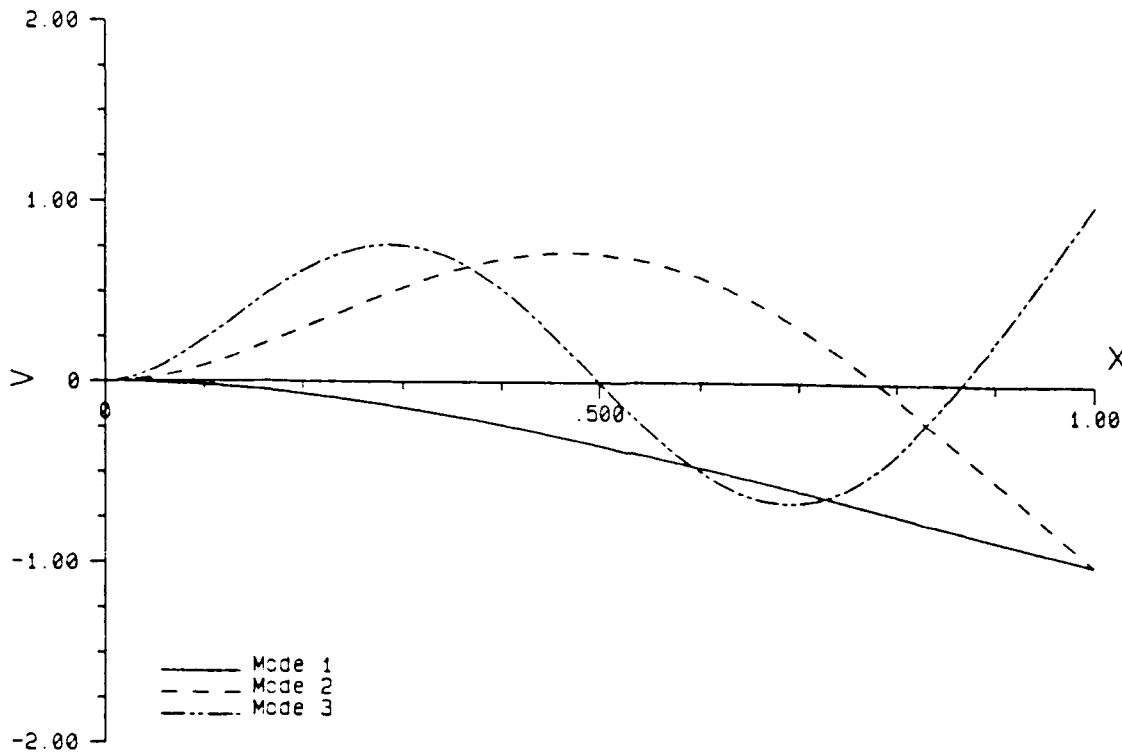


Figure 9. Normalized Lateral Displacement, Base Layer Fixed Free, Constraining Layer Free Free

The maximum damping occurs when the constraining layer is free at both ends, in the third mode. For all modes, damping is higher when the constraining layer is free at both ends, than when it is constrained to rotate with the base layer at $x = 0$. Again, although this runs counter to the initial expectations, it can be explained using the same arguments used in the previous section. Damping is driven by shear strain in the adhesive layer, which is related to the difference in longitudinal displacement of the elastic layers, $u_{e0} - u_{e1}$. Requiring the top elastic layer to rotate with the base layer effectively imposes a zero shear strain boundary condition.

The mode shapes for the first simply supported case are shown in Figures 2 through 4. The mode shapes for the second simply supported case are shown in Figures 13 through 15.

Effect of Permitting Mixed Boundary Conditions on Optimum Design As pointed out earlier, the goal of the design engineer is to maximize the loss factor, for optimum system damping. The effect of mixed boundary conditions on optimum design is of primary concern. In this section, an

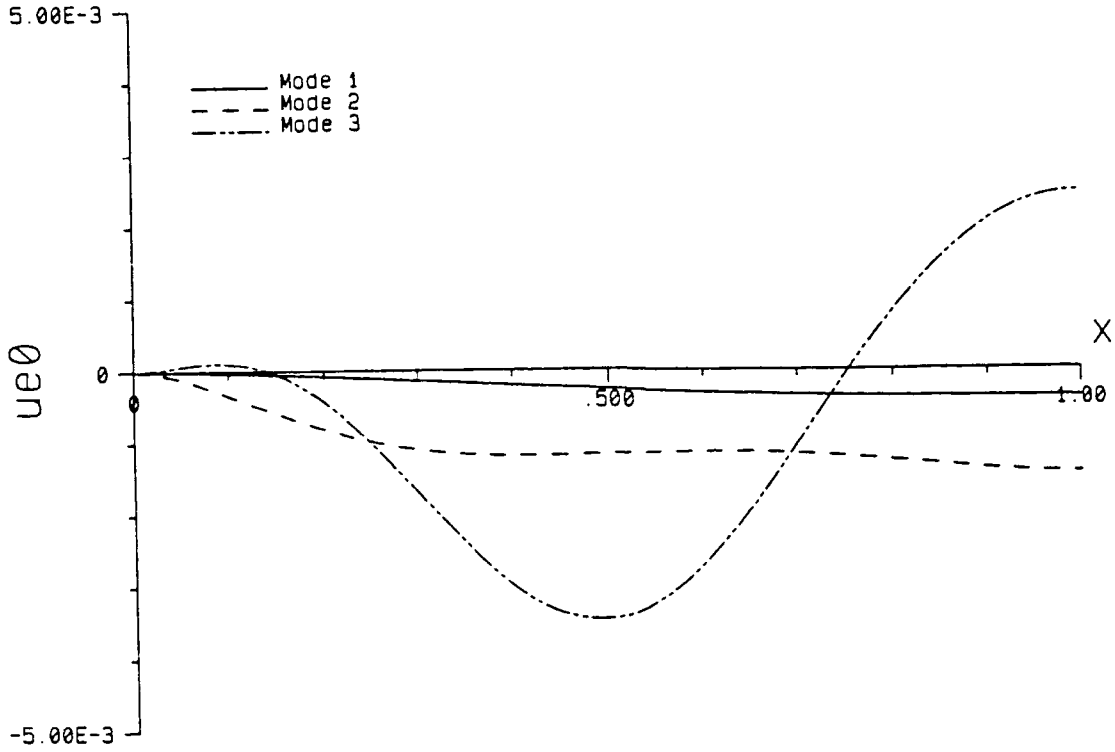


Figure 10. Normalized Longitudinal Displacement of Base Layer, Base Layer Fixed Free, Constraining Layer Free Free

example of an optimum design calculation is shown. Only one variable is considered, the adhesive layer thickness. The loss factor is plotted as a function of adhesive layer thickness for five cases. The first three cases consider loss factors for the cantilever boundary conditions, as predicted by PREDY and BEAM. They are shown in Figures 16 through 18. The fourth and fifth cases are results predicted by BEAM for the two simply supported boundary conditions. They are shown in Figures 19 and 20. The quantity of interest is the thickness at which the loss factor is a maximum. These values are shown in Tables 13 and 14.

For the cantilever boundary conditions, in the higher modes, the curves show a peak for small thicknesses. After decreasing, the loss factor then increases again for large thicknesses. The loss factor would continue to increase, but for magnitudes of thickness which are on the same order of magnitude as the length of the beam. At these values, the rotary inertia terms are no longer negligible, so the equations of motion are not valid (10:221).

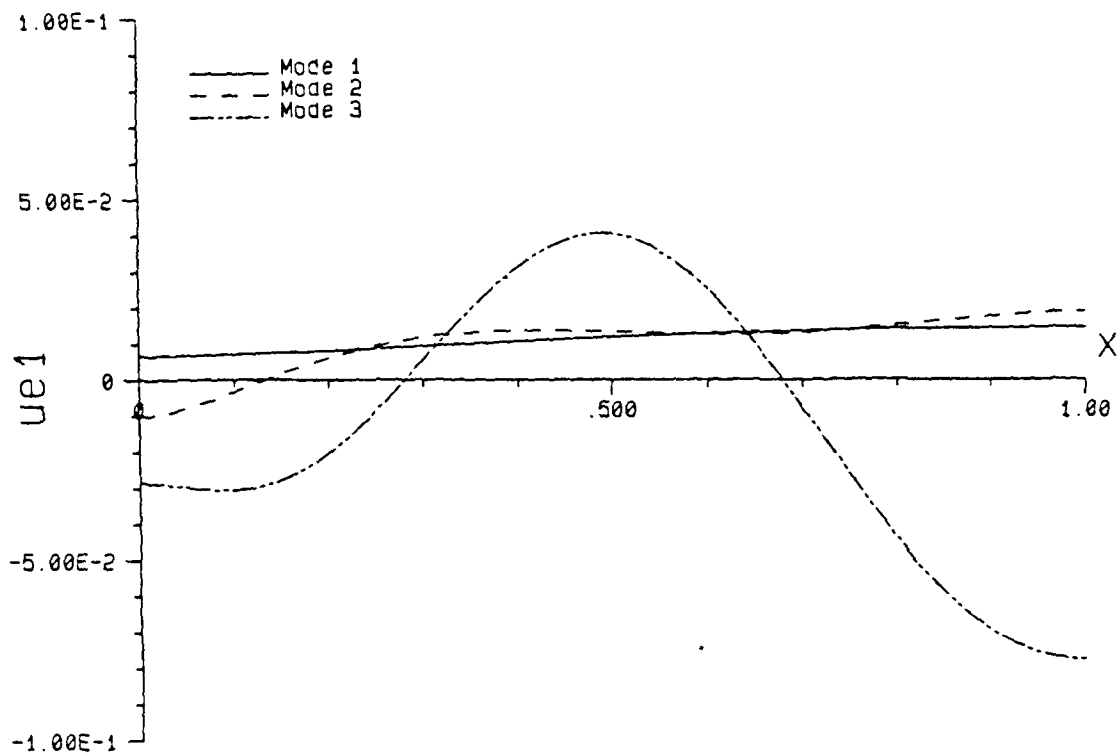


Figure 11. Normalized Longitudinal Displacement of Constraining Layer, Base Layer Fixed Free, Constraining Layer Free Free

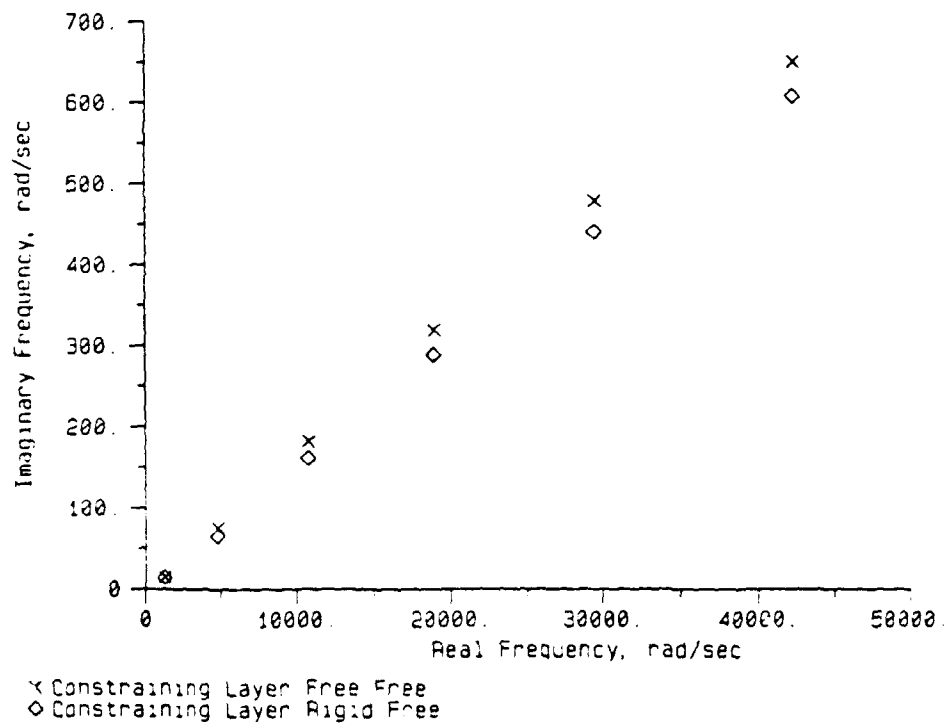


Figure 12. Complex Frequencies for Simply Supported Boundary Conditions

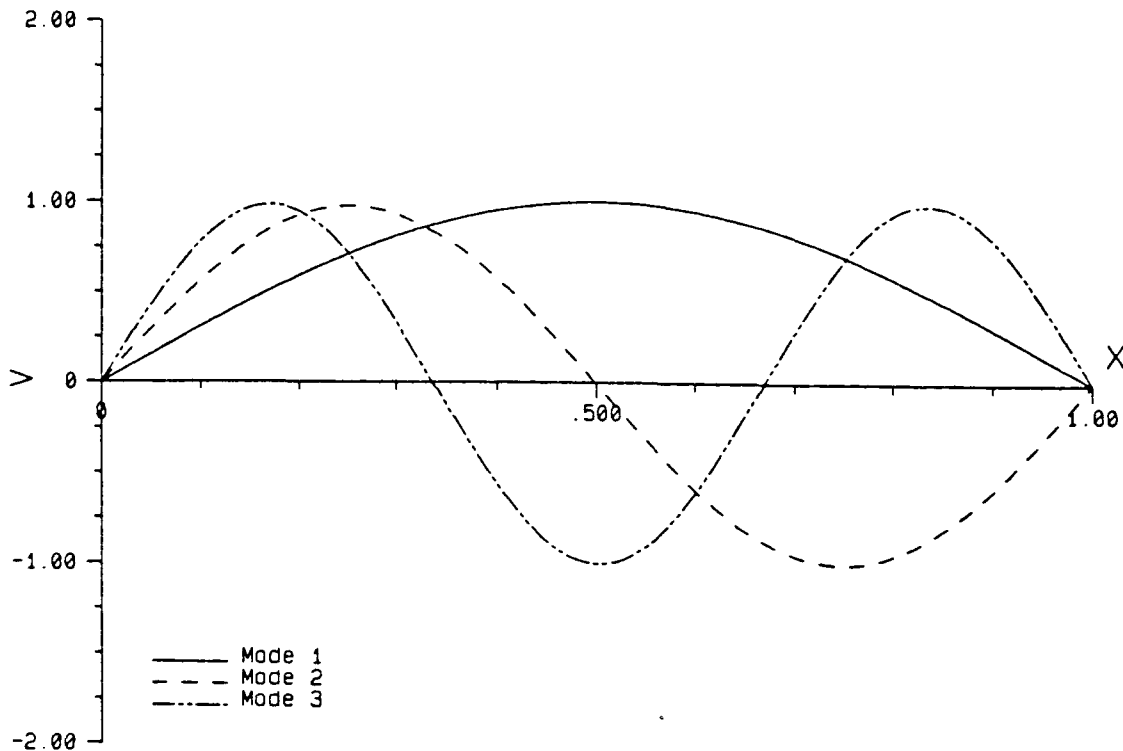


Figure 13. Normalized Lateral Displacement, Base Layer Simply Supported, Constraining Layer Rigid-Free

For the cantilever boundary conditions, all predictions show that there is no optimum for the first mode, and BEAM predicts no optimum for the first three modes. For the fourth through the sixth modes, BEAM predicts the optimum at an order of magnitude larger thickness than does PREDY. For the BEAM predictions, if the constraining layer is fixed at $x = 0$, the optimum thickness is smaller than it would be if the constraining layer is fixed. Figure 21 shows curves for both boundary conditions for the fourth mode, to show the general trend. This shows that fixing the constraining layer at $x = 0$ not only results in a peak at a smaller adhesive layer thickness, but the peak is also higher.

For the simply supported cases, again there is no clear optimum for the lower modes. In the modes where there is a peak, for some modes the different boundary condition has an effect, in other modes it does not.

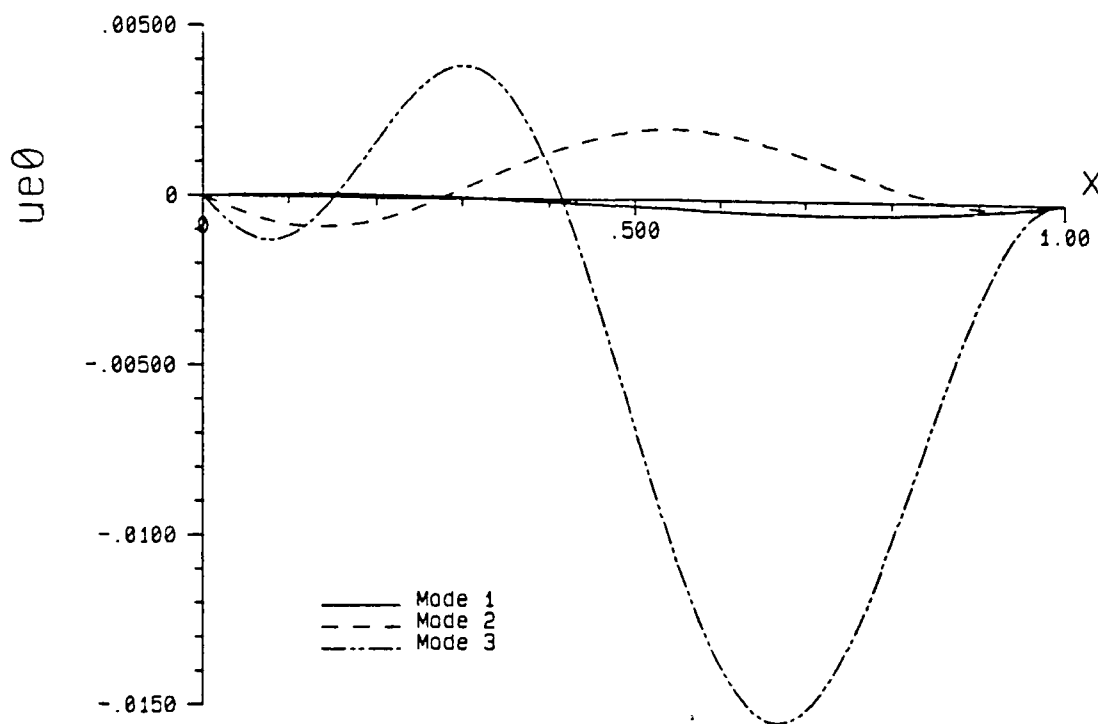


Figure 14. Normalized Longitudinal Displacement of Base Layer, Base Layer Simply Supported, Constraining Layer Rigid-Free

Table 13. Approximate Adhesive Layer Thicknesses for Optimum Damping - Cantilever Boundary Conditions (meters)

Mode	PREDY	BEAM		Diff. between cols 2 and 3
		const. layer fixed free	const. layer free free	
1	no maximum	no maximum	no maximum	
2	0.0002089	no maximum	no maximum	
3	0.0001096	no maximum	no maximum	
4	0.0000759	0.000380	0.000480	26.3 %
5	0.0000575	0.000255	0.000290	13.7 %
6	0.0000479	0.000195	0.000220	12.8 %

Table 14. Approximate Adhesive Layer Thicknesses for Optimum Damping - Simply Supported Boundary Conditions (meters)

Mode	const. layer free free	const. layer rigid free	Diff.
1	no maximum	no maximum	
2	no maximum	no maximum	
3	0.00045	0.00040	11 %
4	0.00028	0.00028	0 %
5	0.00025	0.00020	20 %
6	0.00018	0.00016	11 %

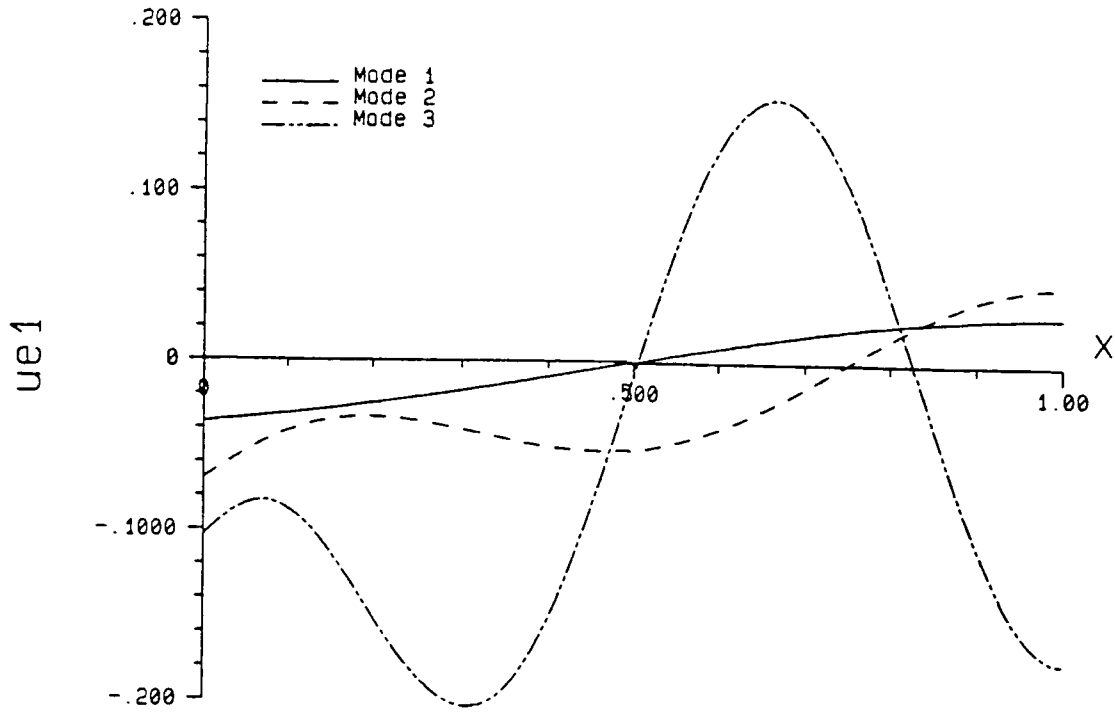


Figure 15. Normalized Longitudinal Displacement of Constraining Layer, Base Layer Simply Supported, Constraining Layer Rigid-Free

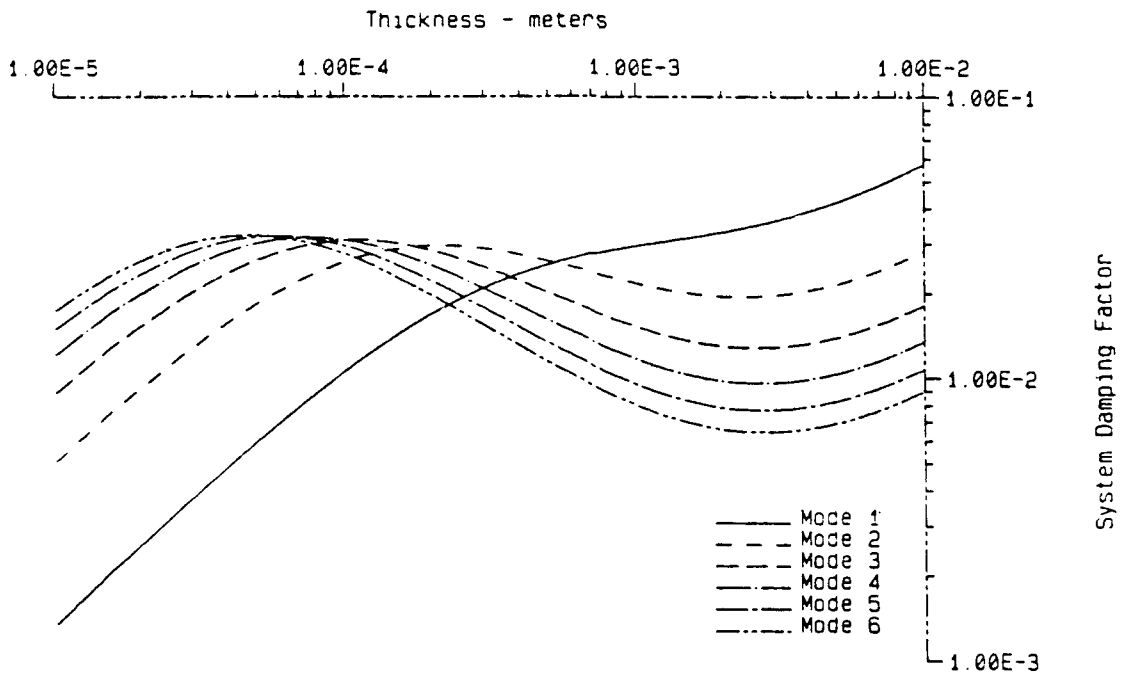


Figure 16. Beam Loss Factor vs. Thickness as Predicted by PREDY - All Layers Fixed-Free

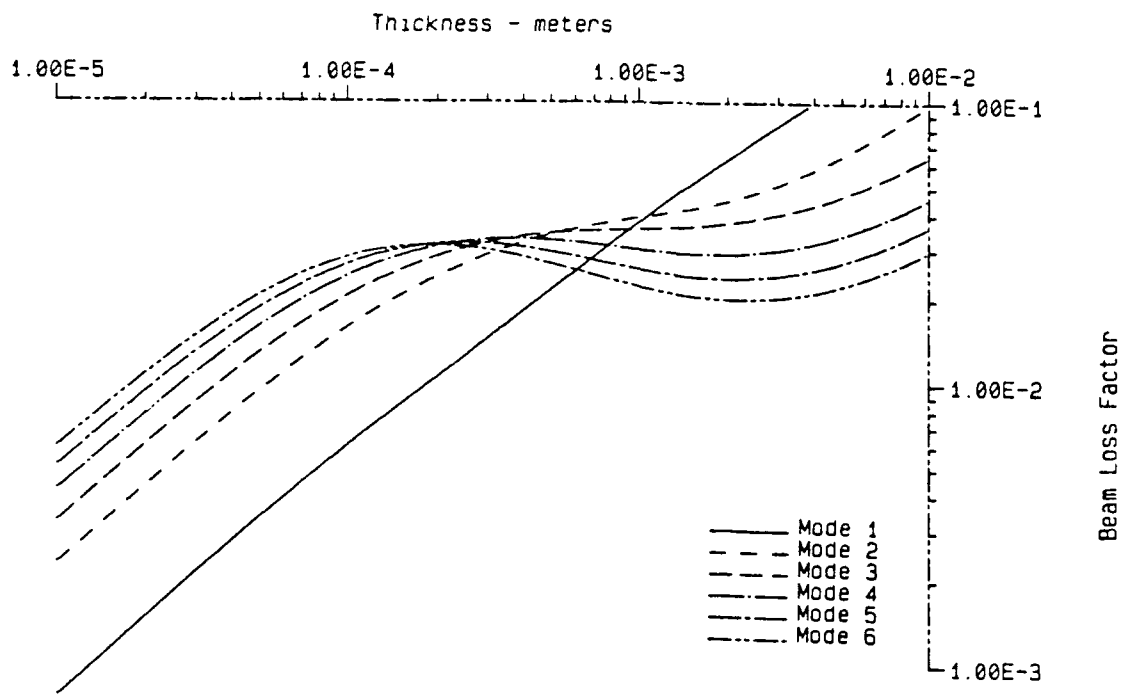


Figure 17. Beam Loss Factor vs. Thickness as Predicted by BEAM - All Layers Fixed-Free

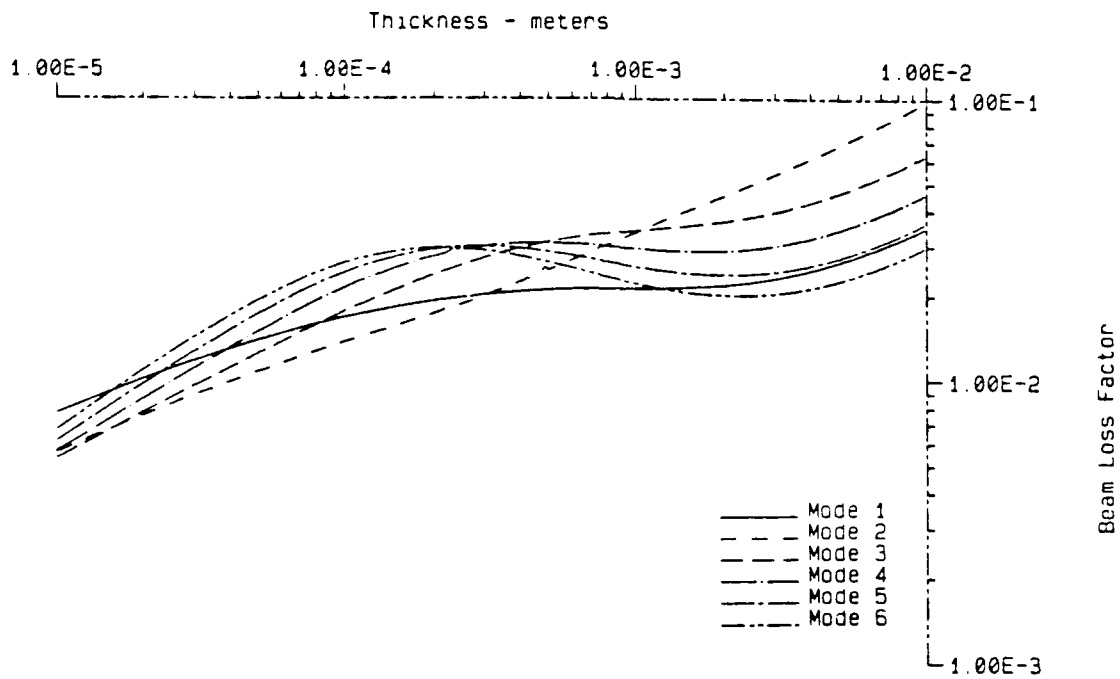


Figure 18. Beam Loss Factor vs. Thickness as Predicted by BEAM - Base Layer Fixed-Free, Constraining Layer Free-Free

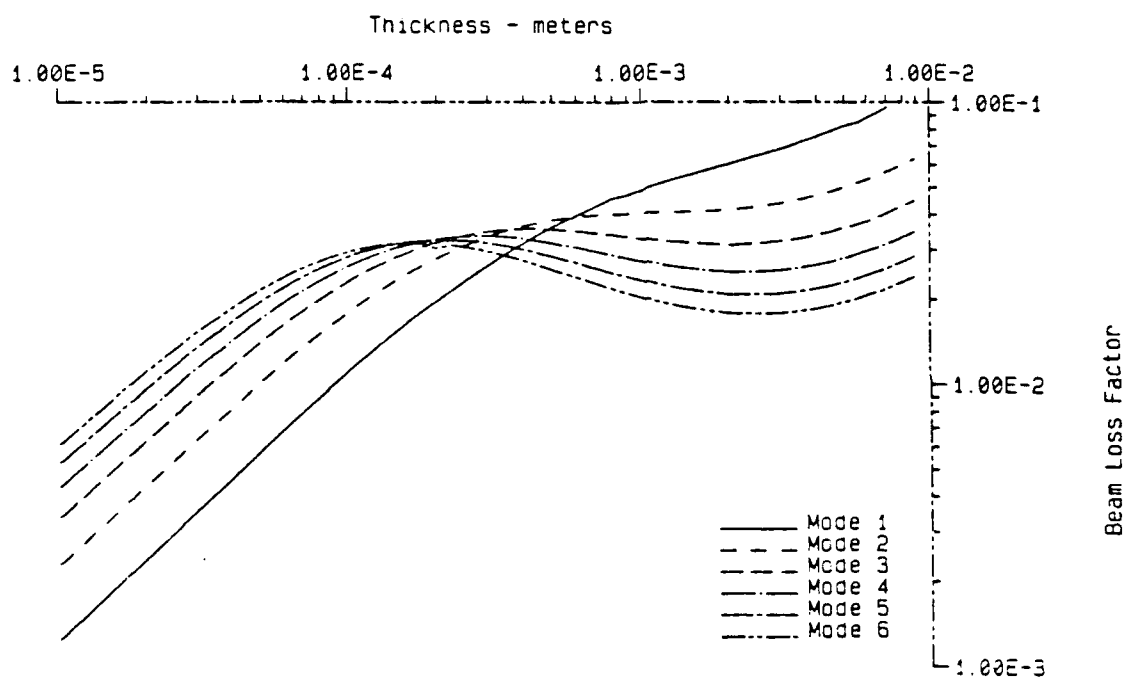


Figure 19. Beam Loss Factor vs. Thickness as Predicted by BEAM - Base Layer Simply Supported, Constraining Layer Free-Free

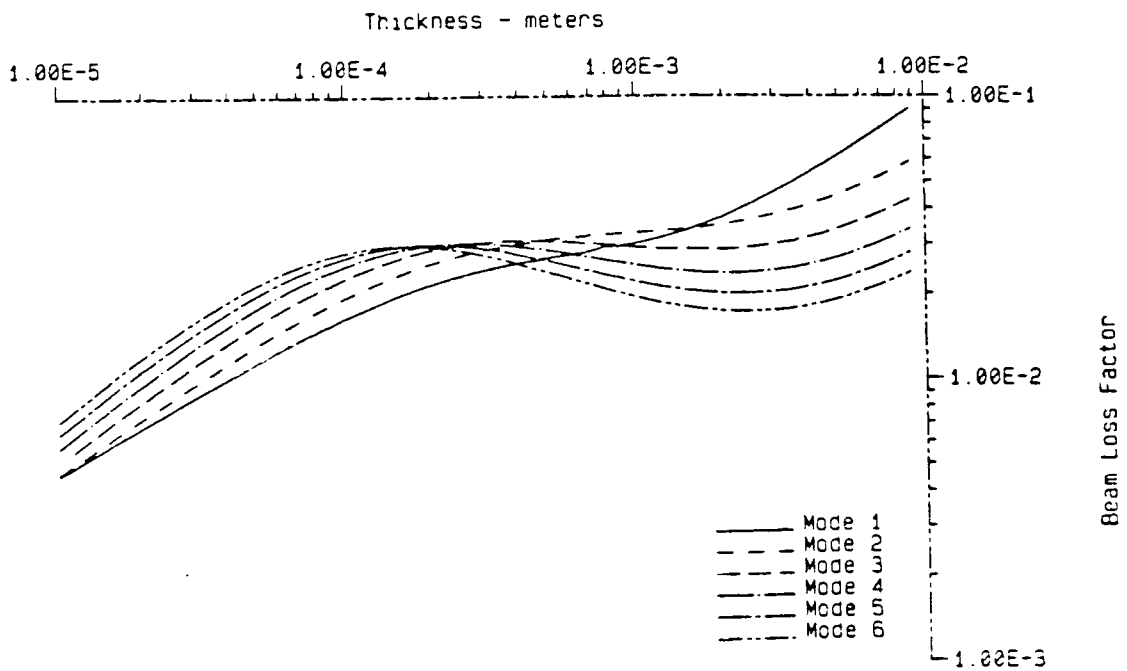


Figure 20. Beam Loss Factor vs. Thickness as Predicted by BEAM - Base Layer Simply Supported, Constraining Layer Rigid-Free

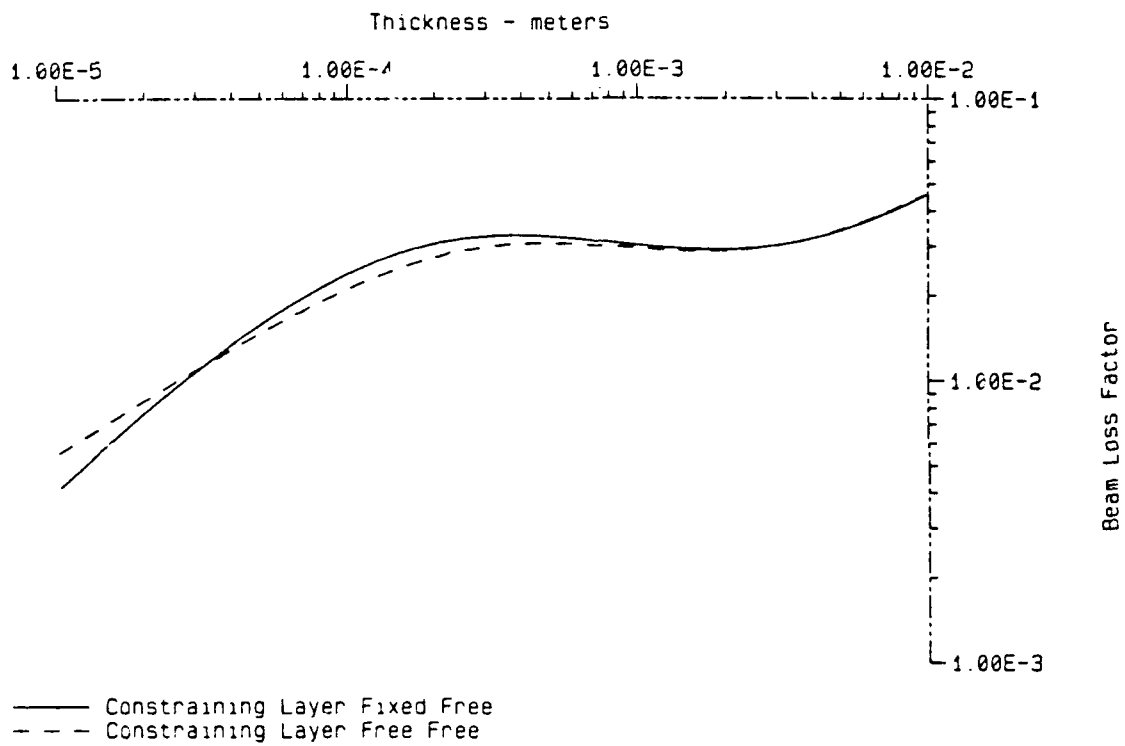


Figure 21. Beam Loss Factor vs. Thickness as Predicted by BEAM - Comparison of Cantilever Boundary Conditions, Mode 4

VIII. Recommendations for Further Research

There are a number of things which should be done to follow up on these results. The formulation should be generalized to more than three layers, and the software modified accordingly. A similar approach should be applied to more complicated geometries, and results compared with previous findings (18:107). A parametric study should be done to gain a more thorough understanding of optimum design configurations.

IX. Conclusion

The equations of motion of a three layer beam were derived using Hamilton's principle. Lateral displacement of the composite beam, and longitudinal displacements of the elastic layers, were considered separately. The formulation resulted in a set of eight boundary conditions which had to be satisfied in order to calculate complex frequencies for damped normal modes. The boundary conditions had nontrivial solutions only when the determinant of the boundary condition matrix was zero.

The boundary conditions matrices were presented for four important cases, selected to illustrate the effects of permitting mixed boundary conditions on frequency and loss factor for the damped normal modes.

Numerical results were presented for a number of test cases for each of the four boundary conditions. First, cases were run for which simple theoretical solutions were available, to determine whether the formulation as presented would correctly predict the frequencies, damping, and mode shapes. The results indicated that the software was performing correctly. Second, some cases were shown to illustrate the effect of permitting the constraining layer to have a different boundary condition than the base layer. For the cantilever case, for all but the first mode, fixing the top layer at $x = 0$ resulted in higher damping than permitting it to be free at $x = 0$. For the simply supported cases, fixing the top layer such that it rotates with the base layer at $x = 0$ resulted in lower damping than permitting the top layer to be free at $x = 0$. Finally, the effects of considering mixed boundary conditions on optimum design was illustrated by calculating loss factor as a function of adhesive layer thickness for all boundary conditions. The thickness at which peak damping occurred shifted dramatically for some modes, and very little or not at all for others. The results as a whole suggest that the optimum design changes depending on whether the top layer has the same boundary conditions as the base layer.

Appendix A. *Notation*

Variables are shown in roughly the order in which they occur in the text. For all quantities, the subscript R denotes the real part, and the subscript I denotes the imaginary part. A dot denotes differentiation with respect to time.

σ = stress

ϵ = strain

E = Young's Modulus, experimentally determined proportionality constant in the relationship of a general, one dimensional, linear elastic material

E_1 = An experimentally determined proportionality constant the Kelvin or Voigt model of viscoelasticity (3:19)

E_2 = An experimentally determined proportionality constant the Kelvin or Voigt model of viscoelasticity (3:19)

t = time

a_m and b_n = empirical proportionality constants in a model of a general, one dimensional, linear viscoelastic material

M and N = the number of derivatives and proportionality constants considered in a particular model

σ_0 = average stress

ϵ_0 = average strain

ω = complex frequency

i = square root of -1

T = temperature

α_T = reduced temperature (17:1-13,503-511)

$A(1) \dots A(6)$ = curve fit parameters in the reduced temperature equation (17:1-13,503-511), Eqn 6, for a given viscoelastic material (17)

$$C_A = \left[\frac{1}{A(2)} - \frac{1}{A(1)} \right]^2$$

$$C_B = \frac{1}{A(2)} - \frac{1}{A(1)}$$

$$C_C = A(5) - A(4)$$

$$D_A = \left[\frac{1}{A(3)} - \frac{1}{A(1)} \right]^2$$

$$D_B = \frac{1}{A(3)} - \frac{1}{A(1)}$$

$$D_C = A(6) - A(4)$$

$$D_E = D_B C_A - C_B D_A$$

$$a = (D_B C_C - C_B D_C) / D_E$$

$$b = (C_A D_C - D_A C_C) / D_E$$

G = Complex shear modulus

f = frequency

$B(1) \dots B(6)$ = curve fit parameters in the shear modulus equation (17:1-13,503-511), Eqn 7, for a given viscoelastic material (17)

x = independant variable measuring distance along the length of the beam

T = total kinetic energy of the beam

M = total mass in a general second order system

u = displacement for a general second order system

k = spring constant or elastic modulus in a general second order system

L = length of the beam

b = width of the beam

η = loss factor

η_v = loss factor of a viscoelastic material

η_b = equivalent loss factor of the layered beam

ρ_{e0} = density of base (elastic) layer

t_{e0} = thickness of the base layer

v_{e0} = lateral displacement of the base layer

u_{e0} = longitudinal displacement of the base layer

ρ_{v1} = density of 1st viscoelastic layer

t_{v1} = thickness of the 1st viscoelastic layer

v_{v1} = lateral displacement of the 1st viscoelastic layer

u_{v1} = longitudinal displacement of the 1st viscoelastic layer

ρ_{e1} = density of 1st elastic layer

t_{e1} = thickness of the 1st elastic layer

v_{e1} = lateral displacement of the 1st elastic layer

u_{e1} = longitudinal displacement of the 1st elastic layer

v = lateral displacement of the composite beam, assuming the lateral displacement of all layers is the same

$(\rho t)_T$ = equivalent areal density (mass per unit area) of the beam

V = total potential energy of the beam

E_{e0} = modulus of elasticity of the base (elastic) layer

G_{v1} = shear modulus of the 1st viscoelastic layer

E_{e1} = modulus of elasticity of the 1st elastic layer

$$d_1 = 1 + (t_{e1} + t_{e0}) / (2t_{v1})$$

$$D_T = (E_{e0}t_{e0}^3) / [12(1 - \nu_{e1}^2)] + (E_{e1}t_{e1}^3) / [12(1 - \nu_{e1}^2)]$$

γ_{v1} = shear strain in the first viscoelastic layer

$$= (u_{e1} - u_{e0}) / t_{v1} + d_1 \partial v / \partial x$$

δ = variational operator

j = index identifying the eight roots of the characteristic equation, Eqn 29, and the constants associated with each root

p_j = a root of the characteristic equation

A_j = average displacement v associated with p_j

B_j = average displacement u_{e0} associated with p_j

C_j = average displacement u_{e1} associated with p_j

$\beta_j = B_j/A_j$

$\gamma_j = C_j/A_j$

$\Psi_j = \beta_j - \gamma_j$

$h_j = d_1(\gamma_j - \beta_j) + d_1^2 t_{v1} p_j - (D_T p_j^3)/G_{v1}$

$\Gamma_j = \gamma_j + t_{v1} d_1 p_j$

BEAM = name of the computer program written as a part of this research effort, to implement the equations presented in the thesis

PREDY = name of the program published in the damping design guide in Reference (16:5-29)

$\lambda = [\omega^2 m / (EI)]^{1/4}$ for a homogeneous cantilever beam (10:224-227)

I = moment of inertia of homogeneous cantilever beam

m = mass per unit length of homogeneous cantilever beam

n = the mode number

D = a constant

$\pi = 3.14159 \dots$

F = a constant

Appendix B. *Description of User Input for BEAM*

To use the software written as part of this research (BEAM), an input data file must be prepared. Following is a description of the format of the input data file, and an explanation of input variables.

The first nine characters of each input data line are ignored by the software. This makes it possible to put the name of the variable on the line, followed by the data, making it easier to keep track of things. The data is then read in free format from columns 10-80. The location of the data on the line is not important, but data must be included for every variable. If a number is zero, it is not sufficient to leave that area blank. A zero must be entered. This is the price which must be paid for the freedom to locate the data anywhere on the line. For data lines on which more than one input variable must be placed, the data must be separated by normal field separators, such as a space or a comma. A description of each of the variables follows. For the physical data, self consistent units should be used.

OUTPUT Name of the file where output data (except plot data) is to be written. It may contain a full pathname, i.e. device:directory/filename

MESSAG Name of the file where messages are to be written. Messages include errors, progress reports, etc. It may contain a full pathname, i.e. device:directory/filename

PLTFIL Name of the file where plot data is to be written. It may contain a full pathname, i.e. device:directory/filename

ICASE A number which identifies the case being run. This number is not used by the program, but it is included in the database output described below.

CDESC A character string describing the case being run. It is not used by the program, but it is included in the database output described below.

IBC A number indicating the boundary condition to be considered. Boundary conditions currently supported are

1. All layers fixed at $x = 0$ and free at $x = L$.
2. All layers fixed at both ends.
3. Base layer fixed at $x = 0$ and free at $x = L$. Constraining layer free at both ends.
4. Base layer pinned at $x = 0$ and at $x = L$. Constraining layer free at both ends.
5. Base layer pinned at $x = 0$ and at $x = L$. Constraining layer rotates with base layer at $x = 0$, and is free at $x = L$.

BCDESC A character string describing the boundary condition. It is not used by the program, but it is included in the database output described below.

PROMPT A logical variable (T or F). If true, the software will ask prompt the user for responses, such as continuing in the event of an error, or closing files, etc. If false, the software does not ask for any user input. This is useful for running in batch mode.

PLOT A logical variable (T or F). If true, the software will write the mode shapes as a function of position to the file PLTFIL in a format which may be read by a plotting package.

MODOUT A logical variable (T or F). If true, the software will write 'mode' data, the constants $A_1 \dots A_6$, B_7 and B_8 to OUTFIL.

VERBC A logical variable (T or F). If true, the software will substitute 'zeros' found back into the boundary condition equations, calculate the error, and write the error to OUTFIL.

SBOUT A logical variable (T or F). If true, the software will write result data in a format which may be read into a database manager. This output only makes sense for a database file which is properly defined. The best way to understand the output is to look at it for a couple of weeks.

ZEROUT A logical variable (T or F). If true, the software will write values of complex frequencies at the relative minima.

UNIFRM A logical variable (T or F). If true, the grid used to search for zeros will be everywhere uniformly spaced. If false, the grid size will increase geometrically from the minimum to the maximum values, resulting in a finer grid nearer the minimum. This should only be used if only the first quadrant in the complex frequency plane is being searched.

WATCH A logical variable (T or F). If true, the software will count iterations and print progress every IPRINT iterations. This is not a good idea if console output is being redirected to a file, as in a batch run. It is very helpful if console is being directed to the terminal, and the run is expected to take a long time.

VARYG A logical variable (T or F). If true, the complex shear modulus will be calculated at each frequency value using the temperature and empirical constants listed below. If false, the temperature and empirical constants are all ignored except GVB1 and GVB2. GVB1 is taken to be the real part of the complex modulus, and GVB2 is taken to be the imaginary part. They are held constant for all values of frequency.

ITERAT A logical variable (T or F). If true, the variable specified by ITVAR will be iterated according to the values in XIT. Note that the entire grid will be searched and all zeros found for every value of ITVAR. This could take a while, so it is a good idea to know how fast the calculations go before attempting to iterate anything.

LOGINC A logical variable (T or F). If false, the values in XIT are used directly for ITVAR. If true, and if ITERAT is true, the variable listed in ITVAR will be incremented 'logarithmically'. In other words, the data points will be equally spaced on a log axis. The values in XIT will be interpreted accordingly. The first value assigned to ITVAR will be

$$10^{x_1}$$

and the maximum value assigned to ITVAR will be

$$10^{x_m}$$

The increment value, x_i will be the difference between the base ten logarithm of successive XIT values. For example, if the user would like to calculate 20 values, from 10 to 1000, equally spaced on a log axis, the three values in XIT would be 1, .1, 3.

ITVAR An integer indicating which variable is to be iterated. The number refers to the physical data listed below. XL is variable 1, EEOR is variable 2, etc. down to XNUE1 which is variable 26.

XIT Three values controlling the iteration of ITVAR. The first number is the minimum value (x_1), the second the increment (x_i), and the third the maximum (x_m).

IPRINT An integer specifying how often progress is to be printed to the console, if WATCH is true. For example, if IPRINT = 1000, the software will print a progress message every 1000 iterations. This is an important safety valve. There are times when the user will want to interrupt program execution. For example, it is easy to inadvertently ask the program to search a grid which would take it several months. There are also times when it is clear that things are not running correctly. In both MS-DOS and AmigaDOS, a control-C interrupt only takes effect when the program is performing terminal I/O. Specifying a reasonable value for IPRINT will force the program to 'come up for air' periodically, and give the user a chance to interrupt it gracefully.

OM0 Two real numbers specifying the starting value for the complex frequency grid. The first number is the real value, the second the imaginary.

OMMAX Two real numbers specifying the ending value for the complex frequency grid. The first number is the real value, the second the imaginary.

NOMEGA Two integers specifying how many points to calculate in the complex frequency grid. The first number specifies how many real values to calculate, the second how many

imaginary values to calculate. In the current implementation, the number of imaginary points is limited to a maximum of 2500, and an unlimited number of real points may be calculated. It would be wise to experiment with a few calculations before asking for a large grid, to get a feel for how fast the computer will work.

DETZER A real number controlling the end of a search for a zero. If the magnitude of the determinant at a zero is less than DETZER, the search terminates.

OMTOL A real number controlling the end of a search for a zero. If the distance between two successive frequency values is less than OMTOL, the search terminates.

NMODES An integer specifying how many zeros are to be printed in the mode shape plot file, PLTFIL. This does not limit the number of zeros which will be found, only the number which will be written to the plot file.

NX For the mode shape plot file, this is the number of X values for which the displacements will be calculated and written. They will be uniformly spaced from $x = 0$ to $x = L$.

XL The length of the beam.

EE0R The real part of the modulus of elasticity of the base layer.

EE0I The imaginary part of the modulus of elasticity of the base layer.

TE0 The thickness of the base layer.

RHOE0 The density of the base layer.

XNUE0 Poisson's ratio for the base layer.

GVA1 Empirical constant A1 used to calculate the shear modulus.

GVA2 Empirical constant A2 used to calculate the shear modulus.

GVA3 Empirical constant A3 used to calculate the shear modulus.

GVA4 Empirical constant A4 used to calculate the shear modulus.

GVA5 Empirical constant A5 used to calculate the shear modulus.

GVA6 Empirical constant A6 used to calculate the shear modulus.

GVB1 Empirical constant B1 used to calculate the shear modulus.

GVB2 Empirical constant B2 used to calculate the shear modulus.

GVB3 Empirical constant B3 used to calculate the shear modulus.

GVB4 Emperical constant B4 used to calculate the shear modulus.

GVB5 Emperical constant B5 used to calculate the shear modulus.

GVB6 Emperical constant B6 used to calculate the shear modulus.

TEMPER The temperature, used to calculate the shear modulus.

TV1 Thickness of the adhesive layer.

RHOV1 Density of the adhesive layer.

EE1R The real part of the modulus of elasticity of the constraining layer.

EE1I The imaginary part of the modulus of elasticity of the constraining layer.

TE1 The thickness of the constraining layer.

RHOE1 The density of the constraining layer.

XNUE1 Poisson's ratio for the constraining layer.

A sample input data file follows. Note that the actual data begins in column ten.

```

OUTPUT = data:test.out
MESSAG = *
PLTFIL = data:test.plt
ICASE = 3
CDESC = damped-beam
IBC = 1
BCDESC = fixed/free
PROMPT = F
PLOT = F
MODOUT = T
VERBC = T
SBOUT = F
ZEROUT = F
UNIFRM = T
WATCH = T
VARYG = T
ITERAT = F
LOGINC = F
ITVAR = 20
XIT =      0.001      0.00154      0.003
IPRINT = 1000
OMO =      10.      -10.

```

OMMAX	=	2800.	10.
NOMEGA	=	25	5
DETZER	=	1.D-20	
OMTOL	=	1.D-14	
NMODES	=	20	
NX	=	100	
XL	=	.254	
EEOR	=	6.89E10	
EEOI	=	0.	
TEO	=	.00508	
RHOEO	=	2770.0	
XNUEO	=	.33	
GVA1	=	335.	
GVA2	=	280.	
GVA3	=	390.	
GVA4	=	.7E-1	
GVA5	=	.1142	
GVA6	=	.3E-1	
GVB1	=	.2E6	
GVB2	=	1200.E6	
GVB3	=	1.885E7	
GVB4	=	.55	
GVB5	=	1.5	
GVB6	=	.1	
TEMPER	=	350.	
TV1	=	.000254	
RHOV1	=	969.0	
EE1R	=	6.89E10	
EE1I	=	0.	
TE1	=	.000254	
RHOE1	=	2770.0	
XNUE1	=	.33	

Appendix C. *Programming Notes for Program BEAM*

The software was written in ANSI standard Fortran 77, and compiled and run on a Commodore Amiga 2500/020 using ABSOFT Fortran (1). The code should be easily portable to other computers with only minor modifications. Nonstandard code generally involved such things as system time calls, and device or filename conventions. Anywhere system dependant code was used, it was noted in the source.

Most of the variables are declared in separate files and placed in common blocks. The common files are then included in each routine which needs access to those variables. This simplifies making changes to common blocks. Syntax of the INCLUDE statment may vary among compilers, as will the filename conventions. The include files also have descriptions of the variables. All variables in COMMON are initialized in a BLOCK DATA subroutine, at the end of the main source file.

To maximize portability, most variables were kept under six characters. Case is significant in the variables in the system time routine, which is machine specific. Accordingly, the compiler was required to consider case significance. To avoid any problems, all code was written in upper case.

The data was collected and maintained in a database. All input and all output data for each 'zero' located in all test cases was kept. The database manager used was Superbase Professional 3.0 (12), but the data can be made available in any of a number of common formats. All the data, uncompressed, occupies approximately 6 megabytes of data. When exported to dBaseIII format and compressed using LHarc, the data occupies two compressed files of approximately 500 kilobytes each. LHarc is a standard, freely redistributable compression routine widely available for most personal computers and mainframes.

Bibliography

1. Absoft Corporation, 2781 Bond Street, Rochester Hills, MI 48309 (313)853-0095. *Fortran 77 Reference Manual*.
2. Bagley, Ronald L. and Peter J. Torvik. "Fractional Calculus in the Transient Analysis of Viscoelastically Damped Structures," *AIAA Journal*, 23(4):918-925 (June 1985).
3. Christensen, R. M. *Theory of Viscoelasticity, An Introduction* (second Edition). Academic Press, Inc., 1982.
4. Conte, Samuel D. and Carl de Boor. *Elementary Numerical Analysis, An Algorithmic Approach*. McGraw Hill, 1980.
5. DiTaranto, R. A. "Theory of Vibratory Bending for Elastic and Viscoelastic Layered Finite-Length Beams," *Journal of Applied Mechanics*, pages 881-886 (December 1965).
6. Higdon, Archie, et al. *Mechanics of Materials* (third Edition). John Wiley & Sons, Inc., 1976.
7. Kerwin, Jr., Edward. M. "Damping of Flexural Waves by a Constrained Visco-Elastic Layer," *Journal of the Acoustical Society of America*, 31:952-962 (July 1959).
8. Mead, D. J. and S. Marcus. "The Forced Vibration of a Three-Layer, Damped Sandwich Beam with Arbitrary Boundary Conditions," *Journal of Sound and Vibration*, 10:163-175 (1969).
9. Meirovitch, Leonard. *Methods of Analytical Dynamics*. McGraw Hill, 1967.
10. Meirovitch, Leonard. *Elements of Vibration Analysis*. McGraw Hill, 1986.
11. Miles, R. N. and P. G. Reinhall. "An Analytical Model for the Vibration of Laminated Beams Including the Effects of Both Shear and Thickness Deformation in the Adhesive Layer," *Transactions of the ASME*, 108:56-64 (January 1986).
12. Precision Software Limited, 6 Park Terrace, Worcester Park, Surrey, England, KT4 7JZ (01)330 7166. *Superbase Professional Database Management Systems*.
13. Rao, D. K. "Frequency and Loss Factors of Sandwich Beams Under Various Boundary Conditions," *Journal of Mechanical Engineering Science*, 20(5):271-282 (1978).
14. Saada, Adel S. *Elasticity Theory and Applications*. Robert E. Krieger Publishing Company, Inc., 1974.
15. Soovere, J. and M. L. Drake. *Aerospace Structures Technology Damping Design Guide, Volume I - Technology Review*. Technical Report AFWAL-TR-84-3089, AFSC/AFWAL, 1985.
16. Soovere, J. and M. L. Drake. *Aerospace Structures Technology Damping Design Guide, Volume II - Design Guide*. Technical Report AFWAL-TR-84-3089, AFSC/AFWAL, 1985.
17. Soovere, J. and M. L. Drake. *Aerospace Structures Technology Damping Design Guide, Volume III - Damping Material Data*. Technical Report AFWAL-TR-84-3089, AFSC/AFWAL, 1985.
18. Torvik, Peter J. "The Analysis and Design of Constrained Layer Damping Treatments," *Damping Applications in Vibration Control*, Torvik, Peter J., editor, November 1980.
19. Torvik, Peter J. "Damping of Layered Materials." In *30th AIAA/ASME/ASCE/AHS/ASC Structures, Structural Dynamics and Materials Conference*, AIAA, April 1989. AIAA 89-1422.
20. Trompette, P., D. Boillot and M. A. Ravanel "The Effect of Boundary Conditions on the Vibration of a Viscoelastically Damped Cantilever Beam," *Journal of Sound and Vibration*, 60(3):345-350 (October 1978).

Vita

Captain Eugene T. Cottle was born on 3 Sep 1958 in Quincy, Washington. He grew up in Trenton, Utah, a small farm community near the Utah Idaho border. He graduated from Sky View High School in Smithfield, Utah, in 1976. He majored in Mechanical Engineering at Utah State University, graduating with a Bachelor of Science in December, 1983. He received his commission through the Reserve Officer Training Corp, and entered active duty in January 1984 at Eglin AFB, FL.

While at Eglin, Captain Cottle served for five years in the Air Force Armament Laboratory. He worked as a project officer for office automation for the first two years. During that time he was responsible for automating management information functions, for upgrading business computer systems, for developing software, and for training employees. In late 1985 he moved to the Strategic Defense Initiative Branch, where he began working on spaced based interceptors. He managed structural analysis and simulation software development contracts for about a year. He then moved to the Electromagnetic Launcher Technology Branch, Analysis and Strategic Defense Division, where he was responsible for the development of data analysis software for the electromagnetic gun test facility. He later purchased and supervised the installation of the site computer system. He acted briefly as system manager for the computer system, before being made section chief of the Technology Development Section. In May 1989 he was selected to attend the School of Engineering, Air Force Institute of Technology.

Permanent Address:

5154 Cobb Drive

Dayton, OH

45431

REPORT DOCUMENTATION PAGE

Form Approved
OMB No. 0704-0180

This report is the property of the Air Force Office of Scientific and Technical Services. It is loaned to your organization; it and its contents are not to be distributed outside your organization.

1. AGENCY USE ONLY (Leave blank) 2. REPORT DATE
Dec 90 3. REPORT TYPE AND DATES COVERED
Master's Thesis

4. TITLE AND SUBTITLE
Damping of Layered Beams With Mixed Boundary Conditions

5. FUNDING NUMBERS

6. AUTHOR(S)
Eugene T. Cottle, Captain, USAF

7. PERFORMING ORGANIZATION NAME(S) AND ADDRESS(ES)
Air Force Institute of Technology, WPAFB OH 45433-6583

8. PERFORMING ORGANIZATION REPORT NUMBER
AFIT/GAE/ENY/90D-5

9. SPONSORING MONITORING AGENCY NAME(S) AND ADDRESS(ES)

10. SPONSORING MONITORING AGENCY REPORT NUMBER

11. SUPPLEMENTARY NOTES

12a. DISTRIBUTION AVAILABILITY STATEMENT
Approved for Public Release; distribution unlimited

12b. DISTRIBUTION CODE

13. ABSTRACT
For many years, viscoelastic materials have been used in damping treatments to control vibration. In order to optimize a damping treatment for maximum damping, a design engineer must be able to predict frequencies of vibration of damped normal modes and loss factors as a function of the design parameters. Theoretical models of layered beams have been developed, but to date, exact solutions have assumed boundary conditions to be the same for all layers. In this thesis, equations of motion for a damped, layered beam are solved for the longitudinal displacement of both elastic layers, as well as the lateral displacement of the composite beam. Test cases were run on a computer to verify the validity of the equations, and to compare results with previously published approximate methods. Results show that the software compares well with theory for cases in which simple theoretical solutions are available. To determine the effect of mixed boundary conditions on design optimization, the system damping factor was calculated as a function of adhesive layer thickness using both the previously published approximate methods and the new formulation. Permitting mixed boundary conditions was shown to significantly effect design optimization.

14. SUBJECT TERMS
Damping, Viscolasticity, Vibration, Dynamics, Structural Dynamics

15. NUMBER OF PAGES
84